separations

MDPI

Review

Purification Technologies for NOx Removal from Flue Gas: A Review

Zihan Zhu [1] and Bin Xu [1,2,*]

[1] State Key Laboratory of Pollution Control and Resource Reuse, College of Environmental Science and Engineering, Tongji University, Shanghai 200092, China
[2] Shanghai Institute of Pollution Control and Ecological Security, Shanghai 200092, China
* Correspondence: binxu@tongji.edu.cn; Tel.: +86-021-6598-1831 (ext. 8016)

Abstract: Nitrogen oxide (NOx) is a major gaseous pollutant in flue gases from power plants, industrial processes, and waste incineration that can have adverse impacts on the environment and human health. Many denitrification (de-NOx) technologies have been developed to reduce NOx emissions in the past several decades. This paper provides a review of the recent literature on NOx post-combustion purification methods with different reagents. From the perspective of changes in the valence of nitrogen (N), purification technologies against NOx in flue gas are classified into three approaches: oxidation, reduction, and adsorption/absorption. The removal processes, mechanisms, and influencing factors of each method are systematically reviewed. In addition, the main challenges and potential breakthroughs of each method are discussed in detail and possible directions for future research activities are proposed. This review provides a fundamental and systematic understanding of the mechanisms of denitrification from flue gas and can help researchers select high-performance and cost-effective methods.

Keywords: flue gas purification; NOx removal; oxidation; reduction; absorption; adsorption

Citation: Zhu, Z.; Xu, B. Purification Technologies for NOx Removal from Flue Gas: A Review. *Separations* **2022**, *9*, 307. https://doi.org/10.3390/separations9100307

Academic Editor: Alena Kubatova

Received: 10 August 2022
Accepted: 10 October 2022
Published: 13 October 2022

1. Introduction

The pollutants produced by power plants, industrial processes, and municipal solid waste incineration mainly include particulate matter, sulfur oxides, and nitrogen oxides (NOx) [1,2]. NOx in flue gas mainly exists in the form of NO (90–95%) and NO_2 (5–10%). NOx emissions can cause a series of health problems, such as eye and throat inflammation, chest tightness, nausea, and headaches, as well as environmental problems, such as ozone depletion, acid rain, haze, photochemical smog, and greenhouse gas emissions [3,4]. Therefore, NOx emissions must be reduced and controlled.

In regard to different combustion stages, NOx control methods can be categorized into pre-combustion, in-combustion, and post-combustion control [5]. For pre-combustion control, the focus is on reducing the nitrogen in the fuel, specifically by selecting a fuel with a low nitrogen content or reducing the nitrogen content of the fuel. The in-combustion control technology, also called low-NOx combustion technology, is mainly used to suppress NOx generation by adjusting operation parameters, modifying burners, etc. [6]. For pre-combustion and in-combustion control methods, only low removal efficiencies can be achieved. Without further countermeasures, most of the exhaust gases from industrial furnaces cannot meet emission standards. Therefore, a post-combustion approach is usually used to achieve a higher NOx reduction [7].

Substantial research has been conducted in developing post-combustion technologies to meet stricter environmental regulations for NOx. Figure 1 presents the statistics of yearly published papers on the topic of NOx purification from flue gas. Table 1 lists currently used purification technologies for NOx removal from flue gas after combustion.

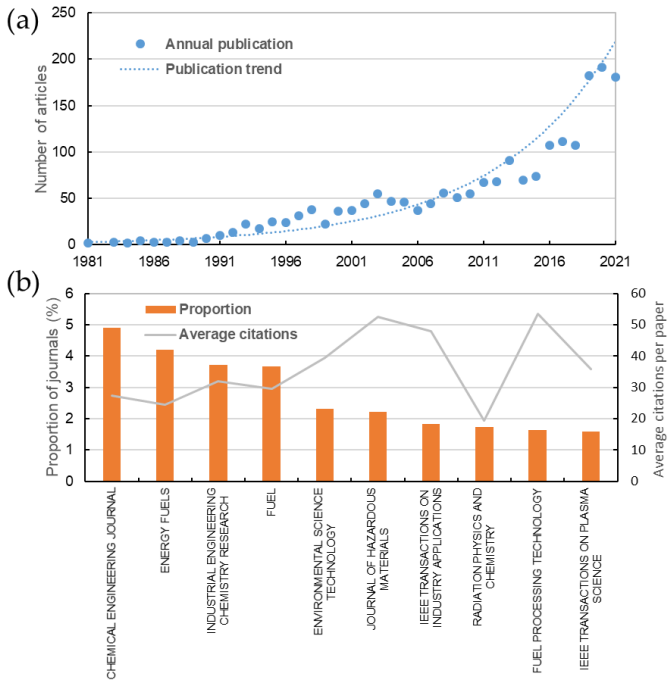

Figure 1. Publication of papers from the last four decades on NOx purification from flue gas. The data were retrieved from the Web of Science database with the topics of "NOx removal" or "DeNOx" and "flue gas" (totally 2078 papers). (**a**) represented the publication trend of papers between 1981 and 2021. (**b**) demonstrated the statistical results of top 10 journals ranked by the number of articles.

Table 1. Post-combustion methods for NOx removal.

Method	Operation Concept	Advantage	Disadvantage	Ref.
Selective catalytic reduction (SCR)	Use gaseous reductants to reduce NOx with catalysts under approximate temperature	High efficiencies	High costs of catalysts Ammonia slip Corrosion of equipment Limited life span of catalyst Large amounts of waste	[8]
Selective non-catalytic reduction (SNCR)	Use gaseous reductants to reduce NOx without catalysts under high temperature	Reliable technology No catalyst used Less equipment investment	High consumption of reactant Ammonia leakage The formation of N_2O and CO Fly ash and unburned carbon increasing	[9]
Absorption	Exposed to liquid absorbents to scrub NOx from gas phase	Simultaneous removal of muti-pollutant Simple operation Stability against inlet gas	High amount of liquid waste Low efficiency Large multi-stage scrubbers	[10]
Adsorption	NOx can be adsorbed by porous solid materials under approximate pressure and temperature	No liquid wastes High purification efficiency Simple equipment	High investment cost Huge equipment	[11]
Non-thermal plasma (NTP)	High-energy electrons excite molecules to generate radicals that can oxidize NOx in a very short time	Low equipment cost No waste Simple operation Useful by-product	High energy cost Low efficiency Low operating pressure	[12]

In this paper, the existing NOx purification methods are summarized and reviewed. In regards to the different transformation approaches (methods causing an increase, decrease,

or no change in the chemical valence of nitrogen), the purification against NOx from flue gas is classified into three types: oxidation methods (N valence increases), reduction methods (N valence decreases), and absorption/adsorption methods (no change in N valence). Furthermore, some innovative methods that are still at laboratory scale, such as non-thermal plasma, are also discussed. The aim of this paper is to present a comprehensive overview of post-combustion NOx purification technologies with different physical state reagents and to help researchers select methods with high performance for NOx removal in specified situations.

2. Oxidation Methods

Regarding the presence of large amounts of insoluble NO in flue gas, oxidizing NO to a much more soluble NO_2 is a highly necessary step, followed by wet scrubbing or dry absorption. In regard to the states of oxidants required for NO oxidation, the reactants are divided into gas oxidants, liquid oxidants, and solid oxidants. The reaction mechanism and the factors affecting the removal efficiency are reviewed.

2.1. Gas Oxidants

Due to the full and effective contact between reactants, gaseous oxidants are widely employed to remove NOx from flue gas. Gas oxidants include oxygen (O_2), ozone (O_3), chlorine species, and non-thermal plasma.

2.1.1. Oxygen (O_2) Oxidants

Oxygen is one of the most common oxidants. Thermodynamically, oxygen can spontaneously oxidize NO to NO_2 and the activation energy for oxidizing NO by O_2 is −4.41 kJ/mol in the temperature range of 270–600 K [13]. However, previous studies have reported that in flue gases from power plants and in industrial processes, such as sintering and waste incineration, the ratio of NO/NOx is still more than 90%, even though there is a considerable proportion of oxygen (3–8%) in the flue gas [14–16].

In oxygenated gaseous environments, the reaction of NO with O_2 proceeds as a third-order reaction [17]:

$$2NO + O_2 \rightarrow 2NO_2 \quad (1)$$

$$-\frac{d[NO]}{dt} = +\frac{d[NO_2]}{dt} = 2\,k\cdot [NO]^2\cdot[O_2] \quad (2)$$

where the rate constant k is dependent on temperature. In untreated flue gases of power plants, the concentration of NOx usually ranges between 200 and 400 ppm [18]. In the tail gas of cement kilns, the concentration of NOx can reach 500–800 ppm or more, and O_2 is concentrated over 8–10% [19]. Therefore, the oxidation rate of NO by O_2 is still low without a catalyst.

Numerous reaction pathways, including a trimolecular reaction, a pre-equilibrium mechanism with a dimer of NO ($(NO)_2$) as an intermediate, and a pre-equilibrium mechanism with NO_3 as an intermediate, have been proposed to explain the homogenous oxidation of NO by O_2 [20].

NO_2 is produced from NO and O_2 at a high pressure and low temperature. Ting et al. [21] investigated the oxidation of NO to NO_2 in the gas phase, absorption in liquid water, and interactions with water vapor at pressures ranging from ambient to 30 bar. As the conversion rate of NO approached 90% over a longer residence period, dry gas oxidation performed well in comparison to global reaction kinetics, which are frequently applied at lower pressures. The study also demonstrated that the NO/NO_2 ratio is mostly unaffected by temperature (25–500 °C).

Although O_2 might directly oxidize NO, the oxidation rate is still constrained. Catalysts, including noble metals, metal oxides/complexes, activated carbon materials, etc., have been extensively studied in recent years. The introduction of diverse catalysts provided active sites, enhancing the reaction between nitric oxide and oxygen and improving the oxidation efficiency. Mn-based catalysts are common catalysts that have recently at-

tracted interest due to their plentiful supply, low cost, easy fabrication technique, and strong thermal stability [22]. The MnO_2 catalysts with various crystal morphologies have shown significant catalysis activity. The γ-MnO_2 catalyst demonstrated the highest activity among the four catalysts (α-, β-, γ-, and δ-MnO_2) and exhibited 91% NO conversion at 250 °C [23]. Gao et al. [24] proposed reaction pathways for NO oxidation by α-, β-, and γ- MnO_2 catalysts, as shown in reactions (3) and (4).

$$\underset{(\square \text{ represents oxygen vacancy, same below})}{\mathrm{Mn}-\square-\mathrm{Mn} \xrightarrow{O_2} 2(-\mathrm{MnO}) \xrightarrow{NO_2(gas)} \mathrm{MnO}-\mathrm{NO}-\mathrm{OMn}} \quad (3)$$

$$\mathrm{MnO}-\mathrm{NO}-\mathrm{OMn} \rightarrow \mathrm{Mn}-\mathrm{O}-\mathrm{Mn}+\mathrm{NO_2} \quad (4)$$

Lattice oxygens contributed to the production of bridging nitrates on the -MnO_2 catalyst. The presence of Mn cations, which were quickly oxidized, led to the conversion of NO and trans-$(N_2O_2)_2$ species [25]. As a result, in addition to reactions (3) and (4) above, the following reactions, reactions (5) and (6), also exist [24]:

$$\mathrm{NO\ (gas)} \xrightarrow{\mathrm{Mn-O\ or\ Mn=O}} \mathrm{MnO}-\mathrm{NO}-\mathrm{OMn} \quad (5)$$

$$\mathrm{NO(gas)} \xrightarrow{Mn^{n+}} \mathrm{NO^-} \xrightarrow{\frac{1}{2}O_2} \mathrm{NO_2(gas)} \quad (6)$$

Yuan et al. [26] discovered that NO adsorbed at oxygen vacancy would be a critical poisoning species and deactivate MnO_2. Possible pathways of NO oxidation based on the Mars–van Krevelen (MvK) mechanism were proposed (as shown in Figure 2). As the favoured pathway showed, the O_2 on oxygen vacancies reacted with the nearby NO absorbed on the Mn cations. An intermediate (ONOO) was formed during this step and then decomposed to NO_2. In this process, the adsorption of oxygen on oxygen vacancies was considered as a decisive step. This result was consistent with previous studies [24,27,28].

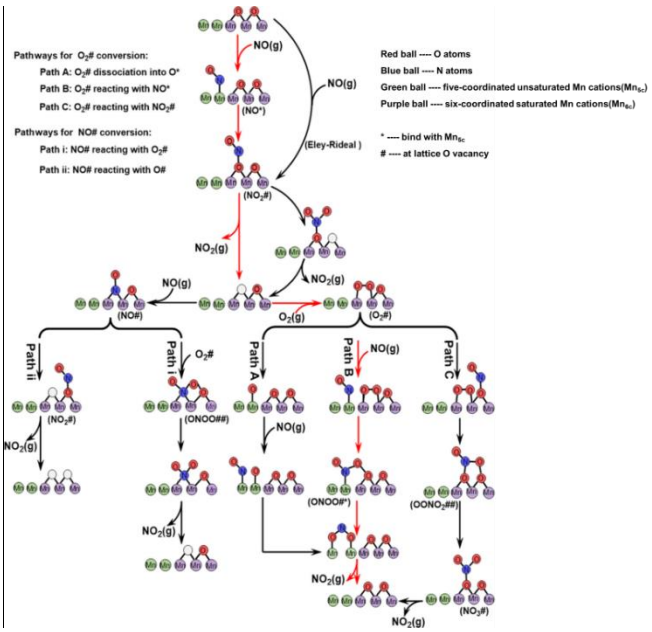

Figure 2. Possible pathways of NO oxidation with the Mars–van Krevelen mechanism occurring on Mn_{5c} site and lattice O on MnO_2. The red pathway represented the favoured mechanism of NO oxidation on MnO_2. Modified from [26] with permission from the American Chemical Society.

2.1.2. Ozone (O_3) Oxidants

O_3 was extensively studied for flue gas purification or emission control due to its high oxidation rate and efficiency, excellent oxidation selectivity, and broad temperature range of use [29].

Recently, an ab initio calculation of quantum chemistry has been used to simulate the oxidation process of NOx. Mok et al. [30] proposed the main 12-step oxidation reaction of NOx oxidation. NO can be directly oxidized by O_3 to NO_2 (reaction (7)) and the rate constant is measured as shown in Equation (8). The main pathways of NOx oxidation by O_3 are shown in Figure 3. However, this 12-step reaction mechanism ignores the interaction of some intermediate gases (such as N_2O, H_2O, HNO_3, etc.).

$$NO + O_3 \rightarrow NO_2 + O_2 \quad (7)$$

$$k = 1.8 \times 10^{-14}\ cm^3\ mol^{-1}\ s^{-1} \quad (8)$$

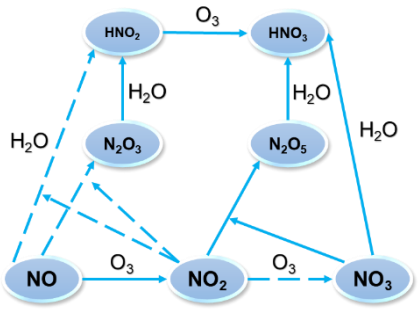

Figure 3. Schematic diagram of the main pathways of NOx oxidation by O_3. Solid lines represent reactions always occurring and dashed lines represent reactions occurring under certain conditions. Adapted from [31].

Several studies have confirmed that the molar ratio affected the mechanism of NO oxidation by O_3 [31–33]. When the molar ratio was less than 1, NO was mainly oxidized to NO_2. When the molar ratio was greater than 1, the oxidation products were NO_2, N_2O_5, and HNO_3. According to Ref. [31], the formation of HNO_3 was due to the presence of H_2O in flue gas. It was also found that the concentrations of N_2O_5 and HNO_3 sharply decreased at temperatures ranging from 120 °C to 180 °C. Therefore, a way to control HNO_3 formation when oxidizing NO by O_3 could be to increase the reaction temperature. The maximum yield of N_2O_5 was produced at 90 °C when the molar ratio of O_3/NO was larger than 1. The most soluble nitrogen oxides, N_2O_5, were the end product of NO oxidation by O_3. As Figure 3 depicted, the products besides N_2O_5 included NO_2, NO_3, N_2O_3, HNO_2, and HNO_3. In particular, NO_3 can rapidly react with NO and decompose to NO_2. Finally, all the NOx species can be transformed into N_2O_5 by the excess amount of O_3. The NOx removal rate reached 96.5% when the molar ratio of O_3/NO NO was 1.8 [34].

Zhou et al. used ozone oxidation and an alkaline counter-flow packed scrubber to investigate ozone decomposition, the oxidation properties of NOx, the removal efficiencies of NOx and SO_2, and the optimal factors [35]. It was found that as the temperature increased and the initial ozone concentration declined, the NOx oxidation efficiency decreased. The NO conversion process was not significantly impacted by SO_2 presence. The most effective additive to lower ozone consumption was $CO(NH_2)_2$. The ideal conditions for reducing SO_2 and NOx were reached, including a temperature of 150 °C, a stoichiometric ratio (0.6) of ozone and NO, and a pH of approximately 8.

2.1.3. Chlorine (Cl_2) and Chlorine Dioxide (ClO_2) Oxidants

Gaseous chlorine species mainly refer to chlorine (Cl_2) and chlorine dioxide (ClO_2). There is little research on its direct application for NO oxidation. As a high-valence gaseous form of chlorine, ClO_2 is more oxidative compared to Cl_2. At temperatures

ranging from 220 to 367 K, the oxidation rate constant of NO to NO_2 by ClO_2 (reaction (9)) was measured and found to be negatively correlated to temperature, with an Arrhenius expression (Equation (10)) [36]:

$$OClO + NO \rightarrow ClO + NO_2 \quad (9)$$

$$k = (1.04 \pm 0.24) \times 10^{-13} \exp[(347 \pm 58)/T] \text{ cm}^3 \text{ mol}^{-1} \text{ s}^{-1} \quad (10)$$

where k represents the reaction constant rate and T represents the temperature of the reaction, K.

Laboratory-scale experiments were carried out to investigate the conversion of NO to NO_2 [37]. It was found that ClO_2 could effectively oxidize NO, and the conversion rate was up to 100%. Cl_2/ClO_2 were often generated on-site using chemical or electrolytic methods from either sodium chlorite or sodium chlorate solutions (reviewed in Section 2.2.3) owing to the shipment and storage security requirements [38]. The application of Cl_2/ClO_2 for de-NOx is usually followed by liquid phase scrubbing technology.

2.1.4. Non-Thermal Plasma (NTP)

Plasma is typically an ionized gas made up of several highly energetic electrons, free radicals, excited species, photons, etc. Electricity-generated plasma is typically divided into two forms: thermal plasma and non-thermal plasma [39]. Since gaseous pollutants might be transformed into inert compounds by free radicals (H•, N•, O•, OH•, O_3•, HO_2•, etc.) in plasma [40], NTP has been expanded to remove NOx in flue gases at atmospheric pressure with significantly less investment, maintaining cost and energy requirements [12]. De-NO and de-SO_2 in a pulsed corona discharge process (PCDP) reactor have been modeled using a mechanism and kinetic scheme, and the model has been confirmed by experimental data. It has been discovered that NO and SO_2 react with oxidizing radicals to form oxides with higher valence states [41]. Table 2 lists the NTP procedures that are currently accessible for NO oxidation from the perspectives of the NTP reactor, additives, gas composition, reaction conditions, and removal efficiency.

Table 2. Experimental conditions and removal efficiencies of available NTP processes for NO oxidation.

NTP Reactor	Gas Composition	Reaction Condition	Maximum Removal Efficiency	Ref.
DBD *	Dry Air/NO (206 ppm)	Energy density: 90 J/L Gas residence time: 3.3 s Reaction temperature: 25 °C Gas flow rate: 1 L/min	99.5%	[42]
	Coal-fired flue gas, NO (200 ppm), SO_2 (250 ppm)	Energy density: 22 J/L Reaction temperature: 75 °C (do*)/90 °C (io*) Gas flow rate: 150 m^3/h	30%(do)/70%(io)	[43]
	N_2/NO (500 ppm)	Energy density: 570 J/L Gas residence time: 0.64 s Gas flow rate: 10 L/min	80%	[44]
	NO (300 ppm), SO_2 (260 ppm), N_2 balance	Catalyst: TiO_2 Pulse frequency: 900 Hz Capacitor-Charging voltage: 12 kV Gas residence time: 1.0 s Reaction temperature: 25 C Gas flow rate: 5 L/min	100%	[45]

Table 2. *Cont.*

NTP Reactor	Gas Composition	Reaction Condition	Maximum Removal Efficiency	Ref.
PCD *	NO (200 ppm), SO_2 (150 ppm), CO (150 ppm), H_2O (10%), O_2 (20%)	Energy density: 7.6 J/L Gas residence time: 1.68 s Reaction temperature: 137 °C Gas flow rate: 1 L/min	65%	[41]
	NO (120 ppm), SO_2 (525 ppm), O_2 (6%), CO_2 (12%), H_2O (3%), N_2 balance	Energy density: 80 J/L Gas residence time: 5.0 s Reaction temperature: 25 °C Gas flow rate: 6 L/min	71%	[46]
	NO (180 ppm), SO_2 (1013 ppm), air balance	Energy density: 45.8 J/L Gas residence time: 4.4 s Reaction temperature: 25 °C Gas flow rate: 72 L/min	40%	[47]
	NO (537 ppm), O_2 (22%), H_2O (RH = 60%), N_2 balance	Energy density: 48.3 J/L Reaction temperature: 25 °C Gas flow rate: 0.3 m^3/h	98.3%	[48]
EBGP *	NO (200 ppm), NO_2 (200 ppm) SO_2 (200 ppm), air balance	Absorbed dose: 20 kGy Reaction ratio: 1:2 Gas residence time:30–40 s Gas flow rate: 1 L/min	94.5%	[49]
	NO (1046 ppm), fuel-combustion flue gas	Wet scrubber: $NaClO_2$ Absorbed dose: 10.9 kGy Gas residence time:11 min Gas flow rate: 200 mL/h	95.03%	[50]

* DBD represents dielectric barrier discharge; PCD represents pulsed corona discharge; and EBGP represents electron beam generated plasma.

As shown in Figure 4, there are often three steps to the elimination of NOx via the collision of electrons with neutral molecules [51]. Within the first nanoseconds, the intense plasma electrons collide with gaseous molecules (with the main components being H_2O, N_2, and O_2), forming primary radicals (HO•, O•, and N•) and ions. Excited molecules, such as oxygen, quickly interact with the main gas after it has been quenched to form more O and HO. Then, the electron–ion and ion–ion reactions continue to produce more secondary radicals with energies higher than those of gas molecules. Although these radicals have a short lifetime under atmospheric pressure and ambient temperature settings, they could convert NOx into HNO_3 in a relatively short period of time (usually 10^{-3} s). These reactions are intense with no apparent sequential response. Finally, before the NH_4NO_3 is collected and used as a fertilizer, the HNO_3 might be neutralized by the ammonia that was generally used in the pulse corona discharge process.

2.2. Liquid Oxidants

For the removal of NOx, wet scrubbing techniques are comparable with other post-combustion technologies. They may also be employed to regulate acid gases and particulate matter simultaneously. As an advanced and stable technology, wet flue gas de-SO_2 (WFGD) contributes to more than 95% of the de-SO_2 capacity and is now being implemented worldwide [52]. However, due to the poor solubility of NO, almost all WFGD technologies are unable to concurrently remove NOx. As a result, upgrading the WFGD to boost the de-NOx function has lately drawn increasing interest. The simultaneous removal of SO_2 and NOx by the oxidation-scrubbing approach is possible if the NO is effectively oxidized, since the solubility of NOx in water increases greatly with its valence. In Table 3, representative oxidants and their redox potentials for liquid phase oxidation are listed.

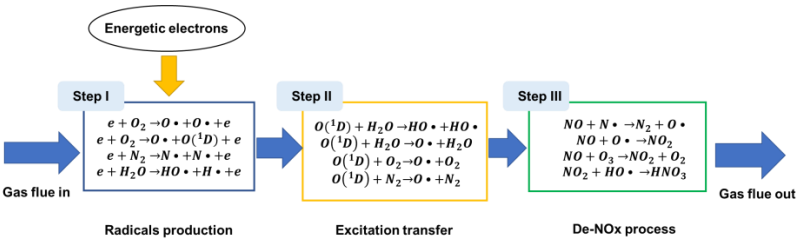

Figure 4. Removal process of NOx by the collision of electrons with neutral molecules. Adapted from [51] with permission from Elsevier, Copyright 2021.

Table 3. Standard oxidation potentials of representative oxidants used in gas–liquid oxidation.

Oxidant	Half-Cell Reaction	Oxidation Potential (eV)	Ref.
Fluorine (F_2)	$F_2 + 2e^- + 2H^+ \rightarrow 2HF$	3.05	[53]
Hydroxyl radical (HO•)	$HO\bullet + H^+ + e^- \rightarrow H_2O$	2.80	[54]
Sulfate radical ($SO_4^-\bullet$)	$SO^{4-}\bullet + e^- \rightarrow SO_4^{2-}$	2.60	[55]
Ozone (O_3)	$O_3 + 2H^+ + 2e^- \rightarrow O_2 + H_2O$	2.07	[53]
Persulfate ($S_2O_8^{2-}\bullet$)	$S_2O_8^{2-}\bullet + 2e^- \rightarrow 2SO_4^{2-}$	2.01	[53]
Peroxymonosulfate (HSO_5^-)	$HSO_5^- + H^+ + 2e^- \rightarrow H_2O + SO_4^{2-}$	1.82	[56]
Hydrogen peroxide (H_2O_2)	$H_2O_2 + 2H^+ + 2e^- \rightarrow 2H_2O$	1.78	[53]
Permanganate (MnO_4^-)	$MnO_4^- + 4H^+ + 3e^- \rightarrow 2H_2O + MnO_2$	1.70	[53]
Chloranion (ClO_3^-)	$2ClO_3^- + 12H^+ + 10e^- \rightarrow 2H_2O + Cl_2$	1.49	[53]
Chloine (Cl_2)	$Cl_2 + 2e^- \rightarrow 2Cl^-$	1.36	[53]
Chromate ($Cr_2O_7^{2-}$)	$Cr_2O_7^{2-} + 14H^+ + 6e^- \rightarrow 7H_2O + 2Cr^{3+}$	1.33	[53]
Molecular oxygen (O_2)	$O_2 + 4H^+ + 4e^- \rightarrow 2H_2O$	1.23	[53]

2.2.1. H_2O_2 Oxidants

Hydrogen peroxide (H_2O_2) is an environment-friendly oxidant. However, the reaction rate of direct NOx oxidation by H_2O_2 is still not ideal [57]. Therefore, it has attracted extensive attention as a precursor of HO• [58]. Transition metal ions (such as Fe^{2+}, Cu^{2+}, and Cr^{3+}), transition metal oxides (such as CrO_3, Al_2O_3), and physical phenomena are widely used to catalyze the conversion of H_2O_2 to HO• [59].

The oxidation of NO by Fenton reagent can be divided into two main steps: (1) oxygen radical generation; and (2) the oxidation of NO. The mechanism reactions are summarized as follows [60,61]:

(1) Oxygen radical generation (Fenton reaction):

$$Fe^{2+} + H_2O_2 \rightarrow Fe^{3+} + OH^- + \cdot OH \quad (11)$$

$$\cdot OH + H_2O_2 \rightarrow H_2O + \cdot O_2H \quad (12)$$

$$Fe^{3+} + \cdot O_2H \rightarrow Fe^{2+} + O_2 + \cdot OH \quad (13)$$

$$Fe^{2+} + \cdot OH \rightarrow Fe^{3+} + OH^- \quad (14)$$

(2) Oxidation by •OH

$$NO + \cdot OH \rightarrow H^+ + NO_2^- \quad (15)$$

$$NO + \cdot OH \rightarrow \cdot H + NO_2 \quad (16)$$

$$NO_2 + \cdot OH \rightarrow H^+ + NO_3^- \quad (17)$$

$$NO_2^- + \cdot OH \rightarrow \cdot H + NO_3^- \quad (18)$$

To increase oxidation efficiency, studies have focused on increasing hydroxyl radical (•OH) generation and H_2O_2 consumption rates [62]. In a lab-scale bubbling reactor, Guo et al. [63] investigated the effects of operating parameters, such as pH value, H_2O_2 concentration, NO inlet concentration, and reaction temperature, on the NO removal efficiency. A significant impact of pH value on NO removal effectiveness was discovered, and the effectiveness of NO removal decreased as the reaction temperature rose. Hao et al. [64] developed an integrated UV-heat/H_2O_2 oxidation system that removed NO by 96.3%.

Since it is challenging to recover the homogeneous catalyst from the solution, the proposed Fenton-like method is a good substitute for the use of transition metals as catalysts. By substituting Fe^{2+} with wet heterogeneous Fenton (-like) oxidation systems (i.e., utilizing metal oxide catalysts or other solid materials to catalyze H_2O_2 to create OH radicals), it is suggested that the Fenton process (homogeneous catalysis) overcame these drawbacks [59,65–67]. Figure 5 illustrates the mechanism of NO removal in the Fe_2O_3-based Fenton-like system [68].

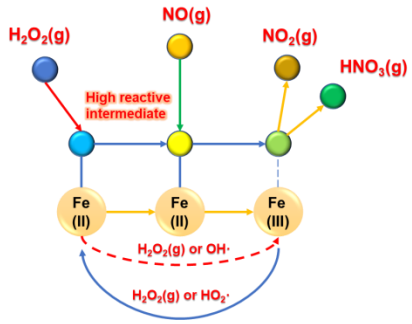

Figure 5. Mechanism of NO removal using Fe_2O_3-based Fenton-like oxidation system. Modified from [60] with permission from Elsevier, Copyright 2019.

2.2.2. Peroxydisulfate/Peroxymonosulfate (PS/PMS) Oxidants

SO_4• has a larger oxidation potential, more selectivity, greater efficiency, and a wider range of pH adaptation than HO•. It is also utilized to oxidize SO_2 and NOx concurrently. The two precursors, peroxydisulfate (PS) and peroxymonosulfate (PMS), typically have standard redox potentials of 2.01 V and 1.82 V, respectively [69]. These two sulfate radicals are kinetically sluggish and stable before stimulation but extremely reactive after stimulation [70]. The corresponding formation mechanisms of SO_4•− are shown in reaction (19) and (20) [71,72].

$$S_2O_8^{2-} \xrightarrow{\text{heat/UV/ultrasound}} 2SO_4^{\bullet -} \quad (19)$$

$$S_2O_8^{2-} + Me_{(aq)}^{(n)+} \rightarrow SO_4^{\bullet -} + SO_4^{2-} + Me_{(aq)}^{(n+1)+} \quad (20)$$

There are many factors influencing the oxidation process of SO_2 and NOx by SO_4^{-}•, such as the temperature, pH value of the solution, and catalyst dosage. NO was oxidized by PS in a bubble column reactor that was run in the semibatch mode [72]. The effects of $Na_2S_2O_8$ concentration, temperature, and solution pH on NO removal efficiency were examined. It was found that the presence of SO_2 significantly increased the NO gas absorption and oxidation. The NO conversions in the presence of SO_2 varied from 77 to 83% with lower temperatures (23 °C and 30 °C).

In the past years, several studies have focused on developing more effective activation techniques for PS/PMS. Chen et al. [73] introduced a combined method with PMS and heating in a rotating packed bed (RPB) pilot reactor. The effectiveness of NO removal exceeded 70%. Liu et al. [74] looked into the variables affecting simultaneous desulfurization and denitrification by using a $NH_4S_2O_8$/UV reactor with a heat exchanger. The elimination of NO with the maximum effectiveness was 96.1%. This might be due to UV light, which sped up the breakdown of $S_2O_8^{2-}$ into SO_4•, combined with water to create •OH, and had a severe oxidizing effect on NO in both cases [75–77]. Liu et al. [74] then conducted research

on the simultaneous absorption of SO_2 and NO by the concurrent thermal activation of $(NH_4)_2S_2O_8$ by an ultrasound and Fe^{2+}. The suitable addition of Fe^{2+} in the $(NH_4)_2S_2O_8$ solution boosted the oxidation and absorption of NO to some extent because the addition of Fe^{2+} might result in the production of free radicals in the $(NH_4)_2S_2O_8$ solution [78]. Figure 6 illustrated the removal mechanism [79]. However, excessive $(NH_4)_2S_2O_8$ would engage in self-consumptive reactions with free radicals SO_4• and •OH, reducing the effectiveness of the NO elimination [69,80].

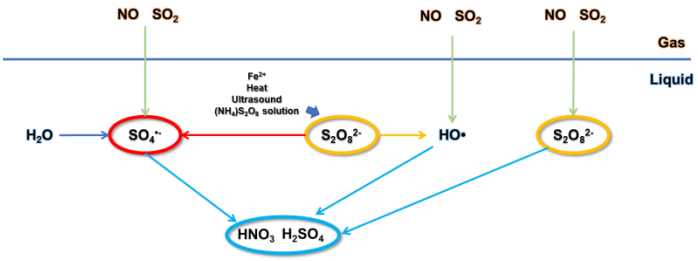

Figure 6. Removal mechanism of NO and SO_2 by ultrasound/Fe^{2+}/heat/$(NH_4)_2S_2O_8$ system. Adapted from [79].

2.2.3. NaClO/ $NaClO_2$ Oxidants

Flue gas contaminants are typically removed using hypochlorite and chlorate due to their high oxidizability. The mechanism of NOx removal was investigated by Liu et al. [81] utilizing UV-assisted $Ca(ClO)_2$ and NaClO aqueous solution in a spray reactor. According to reactions (21) to (24), the direct oxidations of hypochlorite were the auxiliary reactions, while the oxidations of NO by a hydroxyl radical were the primary reactions (25)–(27).

$$HClO \overset{\text{UV light}}{\rightarrow} \cdot OH + \cdot C \quad (21)$$

$$NO + \cdot OH \leftrightarrow HNO_2 \quad (22)$$

$$HNO_2 + \cdot OH \leftrightarrow HNO_3 + \cdot H \quad (23)$$

$$HNO_2 + HClO \leftrightarrow HNO_3 + HCl \quad (24)$$

$$NO + ClO^- \leftrightarrow NO_2 + Cl^- \quad (25)$$

$$3NO_2 + H_2O \leftrightarrow 2HNO_3 + NO \quad (26)$$

$$NO_2 + H_2O \leftrightarrow HNO_3 + HNO_2 \quad (27)$$

The direct removal of NO from flue gas using hypochlorite was not so impressive. Byoun et al. [82] performed the removal tests of NO, SO_2, and Hg^0 in flue gas from an industrial combustion unit using a spray wet scrubber with NaClO at a concentration of 0.1 L/m^3. At a vaporization temperature of 165 °C and a solution pH range of 4.0–6.0, the removal efficiencies of NO were only 50%

A series of studies have been conducted on the factors influencing the removal of NO from flue gas by chlorates. Zhao's [50] research on the removal of NO from diesel engine exhaust using an electron beam and a wet scrubber revealed that the performance of NO oxidation removal went $NaClO_2$ > $NaClO_3$ > NaClO, from high to low. The elimination rate for NOx increased to 95% when CaO_2 was introduced to a $NaClO_2$ solution for oxidation [83]. Hao et al. [84] made a $NaClO_2/Na_2S_2O_8$ compound oxidant to study the oxidation of NO. The maximum NO elimination effectiveness could reach 82.7% under optimal conditions. The effectiveness of NO removal rose with the compound oxidant flow rate, solution pH, and vaporization temperature, but declined with the flue gas flow.

Recently, numerous processes have been studied to improve removal efficiency. Hao et al. [85] proposed a three-region NO oxidation elimination technique with a NO removal effectiveness of 94.5%. Furthermore, it was shown that ClO_2 was quite selective in the oxidation of NO. ClO_2 is more likely to oxidize NO when various contaminants coexist

in the flue gas. The results agreed with Hao's [86] findings after oxidizing NO and Hg^0 with $UV/NaClO_2$, UV/NaClO, $UV/Na_2S_2O_8$, $UV/KHSO_5$, and UV/H_2O_2. In comparison to the others (•OH and SO_4•), the free radicals formed by $UV/NaClO_2$ and UV/NaClO showed higher activity, selectivity, and a better tolerance to the high concentration of SO_2. As a result, chlorate had a high rate of oxidation and was simple to obtain, offering considerable potential for the combined removal of contaminants from flue gases.

3. Reduction Methods

Numerous reductants, including gaseous reductants, liquid reductants, and solid reductants, can convert NO in flue gas to N_2. The reduction process, catalysts, mechanism, and key factors impacting the removal efficiency are reviewed. Table 4 summarizes the typical reductants used for NOx purification from flue gas based on the physical states of these reductants.

Table 4. Typical reductants used for technologies of NOx removal.

Physical State	Reductants	Technologies	Reaction Scheme	Key Factors	Ref.
Gas	Ammonia (NH_3)	SCR	$4NH_3 + 4NO + O_2 \rightarrow 4N_2 + 6H_2O$ $4NH_3 + 6NO \rightarrow 5N_2 + 6H_2O$ $4NH_3 + 2NO + 2NO_2 \rightarrow 4N_2 + 6H_2O$ $8NH_3 + 6NO_2 \rightarrow 7N_2 + 12H_2O$	Temperature window, NH_3/NOx ratio, oxygen concentration, catalyst loading and the type of catalyst support used	[87]
	Hydrogen (H_2)	SCR	$2NO + 4H_2 + O_2 \rightarrow N_2 + 4H_2O$		[88]
	Urea ($CO(NH_2)_2$)	SNCR	$2CO(NH_2)_2 + 4NO + O_2 \rightarrow 4N_2 + 2CO_2 + 2H_2O$	temperature, reagent/flue gas mixing, reagent/NOx ratio and reaction time	[89]
Liquid	Sodium sulfide (Na_2S)	Wet Scrubbing	$2NO_2 + Na_2S \rightarrow N_2 + Na_2SO_4$	Gas–liquid ratio, solution concentration, oxidants concentration, temperature, pH value, reaction time	[30]
	Urea solution	Wet scrubbing	$2HNO_2 + NH_2–CO–NH_2 \rightarrow 2N_2 + CO_2 + 3H_2O$		[90]

3.1. Gas Reductants

The gas phase reduction of NO often involves the use of NH_3/urea, CO, H_2, and HC.

3.1.1. NH_3 and Urea($CO(NH_2)_2$) Reductants

The current gas phase NOx treatment methods are mainly selective catalytic reduction (SCR) and selective non-catalytic reduction (SNCR).

Selective catalytic reduction (SCR) of NOx using ammonia (NH_3) has been extensively investigated. Due to the great efficiency (>90%) and good stability of this technology, post-combustion NOx removal has been applied in numerous industrial applications [91].

It is well known that the main reactions of SCR with NH_3 are as below [92,93]:

$$4NH_3 + 4NO + O_2 \rightarrow 4N_2 + 6H_2O \quad (28)$$

$$4NH_3 + 6NO \rightarrow 5N_2 + 6H_2O \quad (29)$$

$$4NH_3 + 2NO + 2NO_2 \rightarrow 4N_2 + 6H_2O \quad (30)$$

$$8NH_3 + 6NO_2 \rightarrow 7N_2 + 12H_2O \quad (31)$$

Regarding the side reactions, the most frequently employed catalysts have a tendency to produce nitrous oxide (N_2O) at high temperatures (>400 °C). As demonstrated in reactions (32) and (33), which depict the oxidation of NH_3 to NO, the unfavorable oxidizing characteristics of the SCR catalysts became more prominent at temperatures greater than 500°C, hence restricting the maximal NOx conversion [94]. Ammonium nitrate (NH_4NO_3) would be generated at lower temperatures below 200 °C in accordance with reaction (34) [87].

$$4NH_3 + 4NO + 3O_2 \rightarrow 4N_2O + 6H_2O \quad (32)$$

$$4NH_3 + 5O_2 \rightarrow NO + 6H_2O \quad (33)$$

$$2NH_3 + 2NO_2 \rightarrow NH_4NO_3 + N_2 + H_2O \quad (34)$$

Catalysts are one of the most important factors influencing the removal efficiency of SCR, which can directly determine other factors, such as the temperature, residence time, and ratio of NH_3/NOx. Catalysts should possess the following characteristics when selecting appropriate SCR catalysts: a high mechanical strength, high de-NOx activity, operating temperature range, and excellent anti-poisoning. Catalysts of several varieties, including supported noble metals (Pt, Pd, Ag, Au), supported noble/transition metals (Pt/Al_2O_3, Pd/Al_2O_3, Rh/Al_2O_3, Rh/ZSM-5, etc.), supported transition metal oxides (NiO, CO_3O_4, V_2O_5, $Fe3O_4$, MnO_2, etc.), and transition metals (Cu, Fe, Cr, V, Mn, etc.) have been studied [91,95,96].

Mn-based catalysts have been the most widely explored among all transition metals because of their high NOx removal potential at low temperatures [97]. The primary variables that determine the catalytic activity of MnOx are crystallinity, specific surface area, shape, and the oxidation state of Mn [98]. The fact that Mn is a multivalent transition metal allows it to create a variety of stable oxides. $MnO_2 > Mn_5O_8 > Mn_2O_3 > Mn_3O_4 >$ MnO is the order of the MnOx catalysts' activities [99]. The efficiency of NOx removal was improved by increasing the amount of oxygen vacancies on the surface of the catalysts. However, deactivation is a problem for Mn-based catalysts as well. Chemical poisoning, sulfur poisoning, hydrocarbon poisoning, and hydrothermal deactivation are the principal deactivation processes of Mn-based catalysts [100–106]. The performance of Mn-based catalysts against SO_2 poisoning and their high-temperature hydrothermal stability are still subpar, and there are few current studies in this area. Future study could concentrate on enhancing the catalyst's functional elements and creating novel support materials to extend the catalyst's useful life, increase its dependability, and lessen the deactivation of Mn-based catalysts.

Similar to SCR, SNCR also has a broad use, regardless of the cost of its catalysts. With NH_3 acting as the reductant, the reaction temperature window for SNCR typically ranges from 850 to 1100°C. The operating circumstances have an impact on the reduction efficiency. The normal removal efficiency in actual applications is less than 50%. Urea is a preferred agent as an alternative to NH_3 because of its nontoxicity, durability, high performance in a wide temperature range, and low NH_3 slip [9]. The decomposition mechanism of urea is described as follows [93]:

$$NH_2\text{–}CO\text{–}NH_2\ (\text{aqueous}) \rightarrow NH_2\text{–}CO\text{–}NH_2\ (\text{molten}) \quad (35)$$

$$NH_2\text{–}CO\text{–}NH_2\ (\text{molten}) \rightarrow NH_3\ (\text{gas}) + HNCO\ (\text{gas})\ \Delta H^{298} = +186\ \text{kJ/mol} \quad (36)$$

$$HNCO\ (\text{gas}) + H_2O\ (\text{gas}) \rightarrow NH_3\ (\text{gas}) + CO_2\ (\text{gas})\ \Delta H^{298} = -96\ \text{kJ/mol} \quad (37)$$

The overall urea breakdown is depicted in reaction (38).

$$NH_2\text{–}CO\text{–}NH_2 + H_2O \rightarrow 2NH_3 + CO_2 \quad (38)$$

Recently, research on urea-SCR-based catalysts has also been conducted. The NO conversion mechanism on the binary $Cu_{0.5}Mn_{0.5}$/NUAC catalyst was presented and extensively studied after a number of binary catalysts were created [107].

Concerns about handling large amounts of NH_3 include: (I) safety issues, high toxicity, and corrosion; (II) the outlet discharge of unreacted NH_3 to the environment; (III) the formation of ammonium sulfate, a corrosive and sticky liquid that is harmful to combustion and downstream equipment; and (IV) high operating costs [5].

3.1.2. H_2 Reductants

Hydrogen is regarded as a clean fuel and an environmentally favorable substance. As a result, the favored NOx removal technique for catalysts is a low-temperature and

selective catalytic reduction using H_2. H_2 offers a viable solution to meet the criterion of raising emission limits without introducing secondary pollutants [88]. Under conditions of excess oxygen, H_2 has been studied as an effective reducing agent for SCR. Due to its high efficiency, ability to reduce NOx at lower temperatures (<200 °C), high N_2 selectivity, and ability to only produce water, this technology is considered to be environmentally friendly [108].

H_2-SCR technology is particularly useful in industrial settings with access to H_2 gas, such as petrochemical factories and oil refineries. The reactions of NO removal by H_2-SCR in the presence of O_2 are shown as follows [88]:

$$2NO + 4H_2 + O_2 \rightarrow N_2 + 4H_2O \left(\Delta H^{298} = -574.0 \text{ kJ/mol}_{NO}\right) \quad (39)$$

$$2NO + 3H_2 + O_2 \rightarrow N_2O + 3H_2O \left(\Delta H^{298} = -412.0 \text{ kJ/mol}_{NO}\right) \quad (40)$$

$$O_2 + 2H_2 \rightarrow 2H_2O \left(\Delta H^{298} = -241.8 \text{ kJ/mol}_{H_2}\right) \quad (41)$$

$$2NO + H_2 \rightarrow N_2O + H_2O \left(\Delta H^{298} = -170.2 \text{ kJ/mol}_{NO}\right) \quad (42)$$

Catalysts are still the key factor in H_2-SCR. The two primary components of H_2-SCR catalysts are active components and supports. The active components, such as noble metals, bimetallic complexes, and non-noble metals (like Ce and Zr), have been extensively studied [109,110].

In H_2-SCR, noble metals are frequently utilized as catalysts. Noble metals have the ability to degrade H_2. Then the degraded H_2 converts NO into N_2 effectively. Platinum is one of the most frequently utilized noble metals for H_2-SCR (Pt). According to Resitoglu [111], the reaction over the Pt/Al_2O_3 catalyst began at about 90 °C. However, Pt catalysts have a limited selectivity for N_2 and an excellent selectivity for N_2O, despite having significant activity at low temperatures. The type of supports had a significant impact on the catalytic activity of the Pt catalyst (such as Al_2O_3, SiO_2, ZSM5, etc.) [110]. The catalyst activity could be impacted by the acidity and alkalinity of the catalyst. The Pt/SiO_2 catalyst performed better in terms of activity at low temperatures when Al_2O_3 and SiO_2 were compared as supports.

Noble metal catalysts, on the other hand, were poorly resistant to sulfur dioxide, which caused sulfates and sulfites to develop on the catalysts' active sites. Such species eventually caused the SCR to stop working and decrease NO removal at low temperatures [112]. The fundamental drawback of H_2-SCR is the prevalence of expensive supported noble metal catalysts as its active catalysts.

3.1.3. HC Reductants

The SCR of NOx with hydrocarbons(HC) as reducing agents has attracted a great deal of attention [113]. HC-SCR appeared to be a promising technique for the removal of NOx from flue gas [114]. However, the reducibility of CH_4 was significantly lower than that of H_2 and CO, because it was a non-polar, high-bond-energy tetrahedron molecule [115].

The oxidation of NO to surface nitrates and the concurrent oxidation of HC to surface oxygenates are the initial steps in the HC-SCR reaction of NOx. The ensuing reaction between the surface intermediates results in the formation of CN and NCO species. After then, the hydrolysis or oxidation of N_2-containing molecules triggers the production of N_2 and CO_2.

Studies have shown that the surface acidity of catalysts, the oxidation activity of metal ions, and the degree of metal dispersion were crucial variables impacting catalytic activities, even though some aspects of these reaction processes were conflicting. Below are the SCR reactions for NOx emissions utilizing HCs as the reductant [116]:

$$N_2 + O_2 \rightarrow NO_2 \quad (43)$$

$$C_xH_yO_z + NO_2 \rightarrow N_2 + CO_2 + H_2O \quad (44)$$

The small temperature window of HC-SCR in comparison to other de-NOx systems is one of its drawbacks (NSR and urea-SCR). These traits are largely related to hydrocarbons' low selectivity for NOx [117]. Therefore, a range of active catalysts was used in the HC-SCR process to improve the catalytic performance and widen the active temperature window [118,119].

3.1.4. CO Reductants

Carbon monoxide (CO) is recognized as an efficient reagent for NOx reduction due to its cheap cost. Since CO is also created during combustion and coexists in flue gas, CO-SCR technology reduces NOx and CO concurrently, and it is anticipated that using CO as the reducing agent would result in a far more affordable and straightforward feeding system for the NOx abatement process [120].

The following two reactions might take place on the surface of a catalyst based on the catalytic process of the L-H mechanism for supported metal oxide catalysts (M: low-valence-state metal oxide, MO: high-valence-state metal oxide) [121]:

$$MO + CO(g) \rightarrow M + CO_2(g) \quad (45)$$

$$M + NO(g) \rightarrow MO + N_2(g) \quad (46)$$

Other two reactions also take place in the presence of oxygen:

$$M + NO(g) + O_2(g) \rightarrow MO + N_2(g) \quad (47)$$

$$M + O_2(g) \rightarrow MO \quad (48)$$

In addition, the subsequent four reactions (Mx(SO_4)y: metal sulfate) would also take place in the presence of O_2, SO_2, and H_2O [122]:

$$M + H_2O(g) + SO_2(g) \rightarrow M_x(SO_4)_y + H_2(g) \quad (49)$$

$$MO + H_2O(g) + SO_2(g) \rightarrow M_x(SO_4)_y + H_2(g) \quad (50)$$

$$M + O_2(g) + SO_2(g) \rightarrow M_x(SO_4)_y \quad (51)$$

$$MO + O_2(g) + SO_2(g) \rightarrow M_x(SO_4)_y \quad (52)$$

$$M_x(SO_4)_y + CO(g) \rightarrow M + COS(g) + CO_2(g) \quad (53)$$

$$M_x(SO_4)_y + CO(g) \rightarrow MO + COS(g) + CO_2(g) \quad (54)$$

When oxygen, sulfur dioxide, and water vapor are present, reactions (49), (50), (51) and (52) lead to the poisoning and deactivation of the catalyst. It is clear from (53) and (54) that employing CO as a reductant could prevent sulfur dioxide from poisoning catalysts, which would help extend the catalyst's life.

CO might be an advantageous reducing agent for NOx removal utilizing the SCR method due to its poisonous nature [123]. The newly created class of internal combustion engines, such as HCCI (homogeneous charge compression ignition) engines, released relatively large levels of CO, which could be employed to reduce NO [124]. Since it could be produced onsite due to the utilization of coal or natural gas at stationary sources, the expensive steps of purchasing, transporting, and storing the reductant could be eliminated [125].

3.2. Liquid Reductants

Using substances, such as ammonia, urea, sodium sulfide (Na_2S), and others, in aqueous solutions to reduce NOx from flue gas is another de-NOx technique. For instance, the elimination of NOx could be accomplished via an absorption method with the addition of Na_2S as a reductant. Mechanism related is shown in reaction (55) [30]. The majority

of liquid reductants, such as aqueous urea or ammonium salts, often involve the direct reduction of NOx. In real-world applications, liquid reductants are frequently employed as absorbents to take acidic gases from flue gas and fix them with more reductants or oxidants. More detailed relevant trials are required to offer a trustworthy method and development because some outcomes have been disagreed upon or need further validation.

$$2NO_2 + Na_2S \rightarrow N_2 + Na_2SO_4 \quad (55)$$

Studies also put attention on techniques combining NOx oxidation and reduction methods in aqueous solutions. Kim et al. designed and tested a wet packed-bed scrubber with a DBD plasma oxidation process using the reducing agents Na_2SO_3 and Na_2S [126]. With a lower chemical consumption and liquid-to-gas ratio, the results indicated that the Na_2S solution was more suitable than Na_2SO_3.

3.3. Solid Reductants

Polyoxometalates (POMs) have sparked a significant amount of interest from both academic and industrial groups, due to their Bronsted acidity, vast molecule volume, abundant active "lattice oxygen," and pseudo-liquid-phase characteristic [127]. Among the POMs, $H_3PW_{12}O_{40}$ (HPW) stood out among the group thanks to its stronger affinity for the polar NO and NO_2 molecules. The published literature claimed that, in addition to nitrate, the adsorbed NOx also exists in the bulk structure as NOH^+ and N_2O_3 [128]. Yang [129] and Belanger [128,130] completed a series of pioneering works on the adsorption and denitrification performance of HPW. Yang developed a two-step process using $H_3PW_{12}O_{40}$ as a solid catalyst to efficiently reduce NO to N_2 in flue gas without the use of any reducing gas. A total of 70% of the NO in a simulated flue gas was absorbed in the fixed bed at 150 °C at a space velocity of 5000 h^{-1}. A total of 68.3% of the absorbed NO was converted into N_2 at 450 °C. The absorption of NO required the presence of O_2 and H_2O, whereas SO_2 and CO_2 had no impact on either absorption or decomposition. These results were confirmed by McCormick [131] and Zhang [132].

Keggin-type polytungstic acid is one of the most significant POMs and might produce a variety of lacunary structures when the pH of its solution rises. With more internal oxygen atoms exposed, these lacunary POMs could interact with different metals to generate substituted-type saturation structures, which would enhance the surface properties of POMs. Germanium POMs were used as adsorbents and catalysts in a two-step procedure described by Wang et al. [127]. W, Mo, and V derivatives of the Keggin structure were created. A maximum adsorption efficiency of 80% (16.2 mgNO_2/g) and an optimal adsorption temperature of around 230 °C were found for germanium-based POMs.

There are three basic challenges in NO reduction by solid reductants: (1) the efficient NO adsorption on the solid surface; (2) quick NO breakdown and desorption; and (3) the cyclic renewal of the solid reducing agent.

4. Absorption/Adsorption Methods

Along with oxidation and reduction techniques, various liquids and solids could absorb or adsorb NO from flue gas without altering their chemical valence. NO is then desorbed and collected by adjusting pressure, temperature, pH of solution, etc. As a result, the absorption/adsorption process produces pure gas compounds or beneficial by-products. Both liquid phase absorption and solid phase adsorption processes have been thoroughly studied.

4.1. Liquid Absorbents

4.1.1. Alkaline Solution

Alkaline solution absorption was effective for treating exhaust gases that contained more than 50% NO_2. Due to the low solubility of NOx, NOx in alkaline solutions could be transformed into nitrite salts that have a tendency to disintegrate at low pHs and high temperatures [133]. Based on these characteristics, high-valence NOx was often absorbed

using the alkali solution absorption method following oxidation. While the absorption effectiveness and the ratio of NO_2/NO were relatively low, this technology might recycle NOx into chemicals such as nitrite/nitrate and sulfate, which are commercially viable.

The mechanism of NOx absorption in alkaline solutions can be mainly divided into gas-phase equilibrium, gas–liquid equilibrium, and liquid-phase equilibrium. The main reactions are summarized in Table 5 [133].

Table 5. Reactions of NOx absorption from gas phase to liquid phase [133].

Reaction Phase	Equilibrium	Equilibrium Constant Value	Units
Gas	$2NO_2(g) \Leftrightarrow N_2O_4(g)$	-	-
	$NO(g) + NO_2(g) \Leftrightarrow N_2O_3(g)$	-	-
	$NO(g) + NO_2(g) + H_2O(g) \Leftrightarrow HNO_2(g)$	-	-
Gas-liquid	$2NO_2(g) \overset{w}{\Leftrightarrow} 2H^+ + NO_2^- + NO_3^-$	2.44×10^2	$(kmol/m^3)^4/atm^2$
	$N_2O_4(g) \overset{w}{\Leftrightarrow} 2H^+ + NO_2^- + NO_3^-$	3.56×10^1	$(kmol/m^3)^4/atm$
	$N_2O_3(g) \overset{w}{\Leftrightarrow} 2H^+ + 2NO_2^-$	6.14×10^{-5}	$(kmol/m^3)^4/atm$
	$N_2O_5(g) \overset{w}{\Leftrightarrow} 2H^+ + 2NO_3^-$	4.25×10^{17}	$(kmol/m^3)^4/atm$
	$NO_2(g) + NO_2^- \overset{w}{\Leftrightarrow} NO_3^- + NO(g)$	7.43×10^6	-
	$HNO_2(g) \overset{w}{\Leftrightarrow} HNO_2(l)$	-	-
	$3HNO_2(l) \overset{w}{\Leftrightarrow} H^+ + NO_3^- + 2NO(g)$	3.01×10^1	$atm^2/(kmol/m^3)$
Liquid	$HNO_2(l) \overset{w}{\Leftrightarrow} H^+ + NO_2^-$	4.60×10^{-4}	$kmol/m^3$
	$3HNO_2(l) \overset{w}{\Leftrightarrow} H^+ + NO_3^- + 2NO(l)$	1.12×10^{-4}	$kmol/m^3$
	$2H^+ + 3NO_2^- \overset{w}{\Leftrightarrow} NO_3^- + 2NO(l)$	8.46×10^5	$(kmol/m^3)^{-2}$

w represents reactions occurring in presence of water.

For the above reactions, some are dominant. The absorption mechanism of NOx in water and the NaOH solution was depicted in Figure 7 [134]. The overall reactions of NOx absorption in water and the alkaline solution are summarized in reactions (56)–(58):

$$3NO_2 + H_2O \rightarrow 2HNO_3 + NO\uparrow \quad (\text{Water}) \tag{56}$$

$$2NO_2 + 2OH^- \rightarrow NO_3^- + NO_2^- + H_2O \quad (\text{Alkaline solution}) \tag{57}$$

$$NO + NO_2 + 2OH^- \rightarrow 2NO_2^- + H_2O \quad (\text{Alkaline solution}) \tag{58}$$

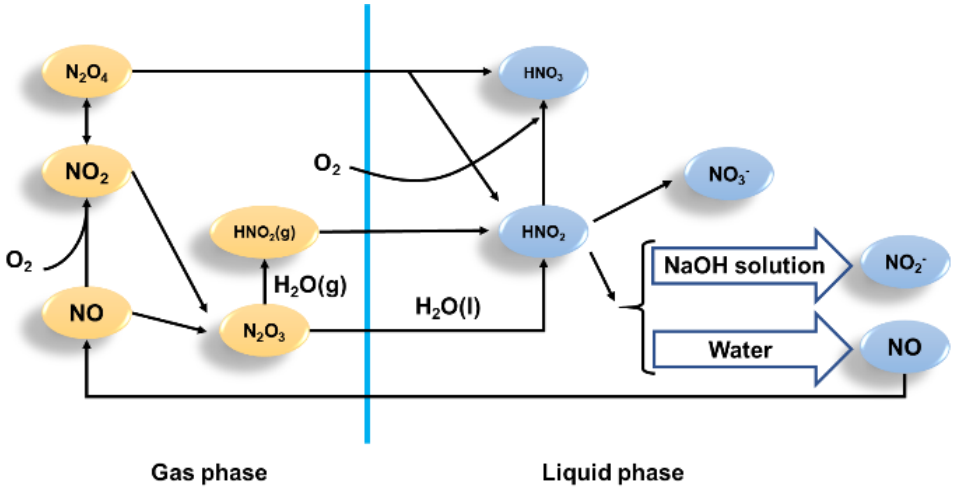

Figure 7. Scheme of NOx absorption into water and NaOH solution.

More attention should be given to reducing physical mass transfer limitations. High mass-transfer rate absorbers need to be developed to alleviate the footprint problems associated with tandem processes [135].

4.1.2. Complex Absorbents

A variety of chelating agents were added to the solution to form a complex in order to increase the removal effectiveness of NO [136]. The solubility of NO in a solution could be greatly improved by adding metal complexation agents (often ferrous and cobalt chelating agents) to the wet scrubbing process, which helps to improve the effectiveness of de-NOx [137].

Chelating substances, such as Fe^{2+}-EDTA (ethylenediaminetetraacetic acid, or EDTA), could improve the solubility of NO by creating stable ferrous-nitrosyl complexes as shown in reactions (59)–(62) [138]. Because Fe^{2+}-EDTA was quickly oxidized to Fe^{3+}-EDTA by O_2, NO, and NO_2 in flue gas (reactions (78) and (79)), the concentration of the active Fe^{2+}-EDTA in the scrubbing solution diminished quickly. The removal effectiveness of NO declined dramatically.

$$NO(g) \rightarrow NO(aq) \quad (59)$$

$$NO(aq) + \left[Fe^{2+} - EDTA\right]^{2-} \rightarrow \left[Fe^{2+} - EDTA(NO)\right]^{2-} \quad (60)$$

$$4\left[Fe^{2+} - EDTA\right]^{2-} + O_2 + 4H^+ \rightarrow 4\left[Fe^{3+} - EDTA\right]^{-} + 2H_2O \quad (61)$$

$$2NO + \left[Fe^{2+} - EDTA\right]^{2-} + 2H^+ \rightarrow N_2O + \left[Fe^{3+} - EDTA\right]^{-} + H_2O \quad (62)$$

The crucial stage in de-NOx by the Fe^{2+}-EDTA solution was the regeneration of Fe^{2+}-EDTA, which involved changing Fe^{3+}-EDTA and Fe^{2+}-EDTA(NO) to Fe^{2+}-EDTA in order to maintain a high NO removal efficiency. Therefore, to effectively reduce Fe^{3+}-EDTA at room temperature, a variety of materials have been used, including activated carbon [139], metal (Se, Zn, Fe, and Al) powders and compounds [140–142], thiosulfates [143], sulfites [144], and bisulfates [145,146]. Reaction (63) shows how iron(0) is used to regenerate Fe^{3+}-EDTA:

$$5Fe + 2\left[Fe^{2+} - EDTA(NO)\right]^{2-} + 12H^+ \rightarrow 2\left[Fe^{2+} - EDTA\right]^{2-} + 5Fe^{2+} + 2NH_4{}^+ + 2H_2O \quad (63)$$

It was found that in the presence of sulfite ($SO_3{}^2$) and hydrosulfite ($HSO_3{}^-$) ions, Fe^{3+} was gradually reduced back to Fe^{2+}, which meant that a specific SO_2 level in the flue gas could promote NO absorption [147]. However, when the SO_2 concentration was excessive, SO_2 might compete with NO for the limited complexant (Fe^{2+}-EDTA) in the solution, thereby reducing the efficiency of de-NOx.

The pH of the solution is another important factor affecting the efficiency of NOx removal. In comparison to both low and high pH values, an intermediate pH often resulted in a higher elimination efficiency [148,149]. It could be concluded that at a pH of around 6.0, the complex formation constant of Fe^{2+}-EDTA was at its highest value. The complex formation constant decreases significantly as the solution becomes more acidic or more alkaline.

4.2. Solid Adsorbents

NOx could also be removed from flue gas directly through adsorption using porous solid adsorbents. The removal efficiency, activation techniques, and factors influencing the efficiency (such as coexisting gases and humidity) were reviewed. In addition to activated carbons and zeolites, metal-organic frameworks (MOFs) have recently been applied.

4.2.1. Activated Carbons (AC)

Due to its high porosity, large surface area, and varied surface chemical properties, activated carbon (AC) is widely utilized industrially as an adsorbent for the control of NOx. Table 6 summarizes the adsorption of NOx with activated carbons from different carbon sources.

Table 6. Adsorption of NOx with activated carbons from different carbon sources.

Carbon Source	Activation Condition	BET Surface (m^2/g)	Reaction Condition	Performance	Ref.
Commercial activated coke	Steam activation (800 °C)	218	Temperature 120 °C, gas flow rate 0.420 Nm3/h, composition of gases: 82.8% N_2, 6.0% O_2, 11.0% H_2O, 1000 ppm NO and 1000 ppm NH_3.	Removal efficiency: 30.4%	[150]
Commercial activated carbon	Steam activation (850 °C), V impregnation	-	Temperature: 200 °C, space velocity: 6500 L/(kg·h), SO_2 (1500 ppm), NO (500 ppm), NH_3 (500 ppm), O_2 (3.4%), H_2O (2.5%), N_2 balance, gas flow rate: 7.00 L/min, contact time: 150 min	Removal efficiency: 70%	[151]
Commercial activated carbon fibers	1 M HNO_3 impregnation for 48 h	1498	Temperature: 200 °C, SO_2 (200 ± 10 ppm), NO (60 ± 3 ppm), air balance, gas flowrate: 0.06 L/min, contact time: 20 min	Removal efficiency: 60%	[152]
Coconut shell	Ionic liquid and KOH impregnation	1114	Sorbent: 3.00 g, temperature: 25 °C, SO_2 (5 ppm), NO_2 (5 ppm), RH (50%), air balance, gas flow rate: 30.00 L/min, contact time: 1200 min	Breakthrough time: 41 min	[153]
Palm shell	CO_2 activation (1100 °C), Ce impregnation	-	Temperature: 150 °C, SO_2 (2000 ppm), NO (500 ppm), O_2 (10%), N_2 balance, gas flow rate: 0.15 L/min, contact time: 300 min	Adsorption capacity: 3.5 mg/g	[154]

Because of the limited physisorption of pollutants on the micropores or surface of AC, the absorbed gas escapes frequently when the temperature or air pressure changes. To enhance catalytic performance, AC must be treated with pre-activation or covering components. The porosity, surface area, and pore size of ACs could be improved via both physical activations (steam and CO_2 activation) and chemical activations (metal oxides, alkaline metals, and acids) [155]. Gao et al. [156] investigated the NO adsorption process using NiO-modified AC/KOH at room temperature. A 5.26 mg/g adsorption capacity and a 95.6% adsorption efficiency were attained. The results showed that a rise in lattice oxygen (O_2- in Ni-O) and OH-/Ox species was responsible for the high removal efficiency of NO.

Flue gas typically contains O_2 and water vapor, which improve NO removal. The adsorbed NO on the surface of AC could be easily oxidized by O_2, then NO_2 could be captured by H_2O to form nitrate acids or salts. The Langmuir–Hinshelwood and Eley–Rideal models provide excellent illustrations of the oxidation pathways of NO over AC [157].

However, the coexistence of SO_2 restricted the NO adsorption, with little NO adsorbed when the SO_2 concentration was more than 700 ppm and the NO adsorption capacity decreased as the SO_2/NO ratio increased [158]. Due to the creation of sulfates and the sulfating of the AC surface, additional downsides have also been documented, including deactivation at low temperatures and poisoning in the presence of SO_2 [159].

The disadvantages mentioned above could be alleviated by impregnating AC with metal oxides (V_2O_5, CuO, Fe_2O_3, MnO_2, Cr_2O_3, and CeO_2), which act as initiators to oxidize NO or reduce it to N_2. For instance, while palm shell activated carbon (PSAC) could remove SO_2, it might remove SO_2 and NO concurrently when it is impregnated with metal oxides, especially when it is impregnated with 10% the weight of CeO_2 [160,161].

The regeneration process played a crucial role in the adsorption technology of NOx. An effective regeneration of the adsorbents ensures the cost-effectiveness and sustainability of the integrated process for the removal of NOx from flue gas. Studies have obtained high regeneration efficiencies (94.2% over five cycles [162] and 94.8% over two cycles [163]) of activated carbon monoliths synthesized with cobalt oxide (ACM-Co_3O_4). Furthermore, Li et al. [164] found that the SCR activity of AC significantly improved after several desulfurization and regeneration cycles, which indicated that the presence of SO_2 could enhance the performance of AC adsorbence after regeneration.

4.2.2. Zeolites

Zeolites have been widely employed as an adsorbent for SOx and NOx removal because of their low cost, nontoxicity, special surface features, and well-defined pore structure.

The mechanism of NOx adsorption removal on the zeolites was studied. Zheng et al. [165] prepared Pd/zeolite as a passive NOx adsorber (PNA) material. It was found that NOx trapping and release were not simple chemisorption and desorption events but involved rather complex chemical reactions. Fundamentally, NO might either physically adsorb by permanently attaching to the surface and forming nitrosyl complexes, or it could reversibly bind to the surface through the binding of nitrogen with the framework cations. Pressure swing adsorption (PSA) allowed the removal of physically adsorbed NO with a minor reduction in pressure, while chemically adsorbed NO could not be removed as readily, even at extremely low pressures [11].

The adsorption performance of zeolites could be effectively improved by surface impregnation. To improve the purification performance of NaX zeolite, ion exchange experiments were conducted with cation K^+, Ca^{2+}, Mn^{2+}, and Co^{2+} by Deng et al. [166]. The result showed that a massive amount of purified NO was degenerated in a reductive way and mainly converted to N_2. Chiu et al. [167] found that $CuCl_2$ impregnation on the zeolite MCM-41 (MCM) increased the NO removal from 62.8% to up to 73%.

Several studies have focused on combined technologies to improve the effectiveness of NO adsorption and remove NOx at the same time. Wang et al. [168] observed NOx storage and reduction with CH_4 over HZSM-5. With this method, a 95% elimination effectiveness of NOx could be attained at room temperature. The effectiveness of NOx removal was kept at over 90% in a cyclic operation. The NOx storage and reduction over HZSM-5 in conjunction with non-thermal plasma in the presence of water were also explored by Wang et al. Due to the competing adsorption of H_2O and NOx on the surface of HZSM-5, the NOx adsorption capacity might be reduced when H_2O is present [169].

4.2.3. Metal-Organic Frameworks (MOFs)

More than 20,000 different MOFs have been created in the last decade. Since their microstructure and constituents are flexible, their shape, size, and functionality can be modified [170]. As for chemisorption, several primary adsorption pathways between SO_2/NOx and the active sites of MOFs were proposed [171,172]. Acid–base interactions, complexation, and hydrogen bonds all played significant roles in the chemisorption among various host–guest interactions. Figure 8 summarizes these important mechanisms of adsorption between NOx and MOFs.

When exposed to industrial exhaust flue gas, very few MOFs have been observed to be stable [173]. Large-scale MOF production has not yet been commercialized. More attention has been dedicated to improving the stability and selective adsorption capability of MOFs in recent years.

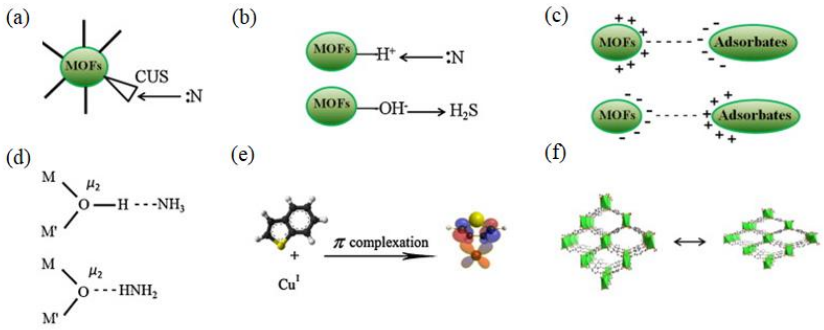

Figure 8. Main mechanisms between NOx and active sites of MOFs. Modified from [171] with permission from Elesvier, Copyright 2013. (**a**) Adsorption on coordinatively unsaturated sites (CUS); (**b**) Acid base interaction; (**c**) Electrostatic interaction; (**d**) Hydrogen bonding; (**e**) π-complex formation; (**f**) Breathing effect.

5. Conclusions and Perspectives

In this paper, the recent literature was reviewed on the purification technologies for NOx removal from flue gas. A novel classification method was proposed from the perspective of changes in the valence of nitrogen (N). According to different transformation approaches (methods causing an increase, decrease, or no change in the chemical valence of nitrogen), the purification against NOx from flue gas was classified into three types: oxidation methods (N valence increased), reduction methods (N valence decreased) and absorption/adsorption methods (no change in N valence). The removal processes, mechanisms, and influencing factors of each method were reviewed according to different physical state reagents.

Oxidation methods utilize gas oxidants (including oxygen (O_2), ozone (O_3), Chlorine (Cl_2)/Chlorine dioxide (ClO_2) and non-thermal plasma (NTP)), and liquid oxidants (including H_2O_2, peroxydisulfate/peroxymonosulfate (PS/PMS), and NaClO/$NaClO_2$). Among these reagents, gas oxidants have attracted a large amount of attention due to their full and effective contact with NOx. However, the high energy consumption of oxidants' generation restricted their large-scale use. Methods utilizing liquid oxidants possessed many advantages, such as available and inexpensive reagents, simple operations, and the simultaneous removal of multi-pollutants. Nevertheless, high oxidation performance still required homogeneous and heterogeneous catalysts to participate in the reaction. Solid catalysts showed their promise in liquid oxidation due to the uncomplicated recovery from aqueous solutions.

Reduction methods were widely applicable in most industrial situations. Much research has been focused on the design and development of more efficient, more durable catalysts that is more resistant to H_2O and SO_2. Liquid reductants were generally utilized after the oxidation of NOx into NO_2 to ensure a high reduction efficiency. Recently, solid reductants have attracted interest from both academic and industrial groups. For instance, $H_3PW_{12}O_{40}$ (HPW) was reported to reduce NO without any reducing gas.

Absorption/adsorption methods provided an effective way to transfer NOx from the gas phase to the liquid/solid phases. However, due to the extremely low solubility of NO in aqueous solutions, pre-oxidation is necessary to make the ratio of NO_2/NOx exceed 50% beyond alkaline absorption. Regarding solid adsorption methods, porous materials, such as activated carbon, zeolites, and metal–organic frameworks (MOFs) were widely studied. According to the proposed mechanisms, increasing the acidity or alkalinity of the adsorbent surface and covering it with metal oxides can dramatically improve the performance of NO adsorption. Therefore, the development of adsorbent modification methods with a higher performance and more detailed mechanisms of the behavior between NOx and adsorbents needs to be further studied.

Author Contributions: Conceptualization, Z.Z. and B.X.; methodology, Z.Z.; investigation, Z.Z.; data curation, Z.Z.; writing—original draft preparation, Z.Z.; writing—review and editing, Z.Z. and B.X.; visualization, Z.Z.; supervision, B.X.; funding acquisition, B.X. All authors have read and agreed to the published version of the manuscript.

Funding: This research was funded by National Key R&D Program of China (No. 2019YFC1904001) and the Natural Science Foundation of Shanghai (21ZR1468000).

Data Availability Statement: Not applicable.

Acknowledgments: This study was partially sponsored the Foundation of State Key Laboratory of Pollution Control and Resource Reuse (Tongji University), China, (No. PCRRE), and the Shanghai Institute of Pollution Control and Ecological Security.

Conflicts of Interest: The authors declare no conflict of interest.

References

1. Li, H.-M.; Zhang, N.; Guo, X.; Dou, M.-Y.; Feng, Q.; Zou, S.; Huang, F.-C. Summary of Flue Gas Purification and Treatment Technology for Domestic Waste Incineration. *IOP Conf. Ser. Earth Environ. Sci.* **2020**, *508*, 012016. [CrossRef]
2. Lin, F.; Wang, Z.; Zhang, Z.; He, Y.; Zhu, Y.; Shao, J.; Yuan, D.; Chen, G.; Cen, K. Flue gas treatment with ozone oxidation: An overview on NO_x, organic pollutants, and mercury. *Chem. Eng. J.* **2020**, *382*, 123030. [CrossRef]
3. Shan, W.; Yu, Y.; Zhang, Y.; He, G.; Peng, Y.; Li, J.; He, H. Theory and practice of metal oxide catalyst design for the selective catalytic reduction of NO_x with NH_3. *Catal. Today* **2021**, *376*, 292–301. [CrossRef]
4. Yuan, B.; Mao, X.Z.; Wang, Z.; Hao, R.L.; Zhao, Y. Radical-induced oxidation removal of multi-air-pollutant: A critical review. *J. Hazard. Mater.* **2020**, *383*, 121162. [CrossRef] [PubMed]
5. Gholami, F.; Tomas, M.; Gholami, Z.; Vakili, M. Technologies for the nitrogen oxides reduction from flue gas: A review. *Sci. Total Environ.* **2020**, *714*, 136712. [CrossRef] [PubMed]
6. Jing, W.; Changjian, L.; Haibo, W.; Ping, J.; Zhiyu, L.; Fanfei, M. Research progress of low-NO_x combustion technology for boilers. *Clean Coal Technol.* **2022**, *28*, 99–114. [CrossRef]
7. Skalska, K.; Miller, J.S.; Ledakowicz, S. Trends in NO_x abatement: A review. *Sci. Total Environ.* **2010**, *408*, 3976–3989. [CrossRef] [PubMed]
8. Sun, Y.; Zwolińska, E.; Chmielewski, A.G. Abatement technologies for high concentrations of NO_x and SO_2 removal from exhaust gases: A review. *Crit. Rev. Environ. Sci. Technol.* **2016**, *46*, 119–142. [CrossRef]
9. Javed, M.T.; Irfan, N.; Gibbs, B.M. Control of combustion-generated nitrogen oxides by selective non-catalytic reduction. *J. Environ. Manag.* **2007**, *83*, 251–289. [CrossRef]
10. Guo, R.-T.; Hao, J.-K.; Pan, W.-G.; Yu, Y.-L. Liquid Phase Oxidation and Absorption of NO from Flue Gas: A Review. *Sep. Sci. Technol.* **2015**, *50*, 310–321. [CrossRef]
11. Rezaei, F.; Rownaghi, A.A.; Monjezi, S.; Lively, R.P.; Jones, C.W. SO_x/NO_x Removal from Flue Gas Streams by Solid Adsorbents: A Review of Current Challenges and Future Directions. *Energy Fuels* **2015**, *29*, 5467–5486. [CrossRef]
12. Ma, S.; Zhao, Y.; Yang, J.; Zhang, S.; Zhang, J.; Zheng, C. Research progress of pollutants removal from coal-fired flue gas using non-thermal plasma. *Renew. Sustain. Energy Rev.* **2017**, *67*, 791–810. [CrossRef]
13. Atkinson, R.; Baulch, D.L.; Cox, R.A.; Crowley, J.N.; Hampson, R.F.; Hynes, R.G.; Jenkin, M.E.; Rossi, M.J.; Troe, J. Evaluated kinetic and photochemical data for atmospheric chemistry: Volume I—gas phase reactions of O_x, HO_x, NO_x and SO_x species. *Atmos. Chem. Phys.* **2004**, *4*, 1461–1738. [CrossRef]
14. Shugen, L.; Binh, N.; Ting, L. Production and Control of NO_x in Sintering or Pelletizing Process. *Sichuan Environ.* **2016**, *35*, 17–22. [CrossRef]
15. Zhao, B.; Su, Y. Process effect of microalgal-carbon dioxide fixation and biomass production: A review. *Renew. Sustain. Energy Rev.* **2014**, *31*, 121–132. [CrossRef]
16. Fang, P.; Tang, Z.; Xiao, X.; Huang, J.; Chen, X.; Zhong, P.; Tang, Z.; Cen, C. Using sewage sludge as a flue gas denitration agent for the cement industry: Factor assessment and feasibility. *J. Clean. Prod.* **2019**, *224*, 292–303. [CrossRef]
17. Gershinowitz, H.; Eyring, H. The Theory of Trimolecular Reactions1. *J. Am. Chem. Soc.* **1935**, *57*, 985–991. [CrossRef]
18. Liang, J.; Lu, L.; Liu, L. Study on Pollutant Quantity of Low Calorific-value Gas Power Plant. *Sci. Technol. Eng.* **2013**, *13*, 9587–9591.
19. Cai, S. Exploring technical ways to reduce NO_x emissions from cement kilns in China. In Proceedings of the Second Summit Forum on Energy Saving, Emission Reduction and Cleaner Production Control Technology in Cement Industry—Special Session on Denitrification and Dust Removal Technology in Cement Industry, Jinan, China, 16–18 April 2013; pp. 36–39.
20. Tsukahara, H.; Ishida, T.; Mayumi, M. Gas-Phase Oxidation of Nitric Oxide: Chemical Kinetics and Rate Constant. *Nitric Oxide* **1999**, *3*, 191–198. [CrossRef]
21. Ting, T.; Stanger, R.; Wall, T. Laboratory investigation of high pressure NO oxidation to NO_2 and capture with liquid and gaseous water under oxy-fuel CO_2 compression conditions. *Int. J. Greenh. Gas Control* **2013**, *18*, 15–22. [CrossRef]

22. Chen, H.; Wang, Y.; Lyu, Y.-K. High catalytic activity of Mn-based catalyst in NO oxidation at low temperature and over a wide temperature span. *Mol. Catal.* **2018**, *454*, 21–29. [CrossRef]
23. Chen, H.; Wang, Y.; Lv, Y.-K. Catalytic oxidation of NO over MnO_2 with different crystal structures. *RSC Adv.* **2016**, *6*, 54032–54040. [CrossRef]
24. Gao, F.; Tang, X.; Yi, H.; Chu, C.; Li, N.; Li, J.; Zhao, S. In-situ DRIFTS for the mechanistic studies of NO oxidation over α-MnO_2, β-MnO_2 and γ-MnO_2 catalysts. *Chem. Eng. J.* **2017**, *322*, 525–537. [CrossRef]
25. Hadjiivanov, K.; Knozinger, H. Species formed after NO adsorption and NO+O-2 co-adsorption on TiO_2: An FTIR spectroscopic study. *Phys. Chem. Chem. Phys.* **2000**, *2*, 2803–2806. [CrossRef]
26. Yuan, H.; Chen, J.; Guo, Y.; Wang, H.; Hu, P. Insight into the Superior Catalytic Activity of MnO_2 for Low-Content NO Oxidation at Room Temperature. *J. Phys. Chem. C* **2018**, *122*, 25365–25373. [CrossRef]
27. Bhatia, D.; McCabe, R.W.; Harold, M.P.; Balakotaiah, V. Experimental and kinetic study of NO oxidation on model Pt catalysts. *J. Catal.* **2009**, *266*, 106–119. [CrossRef]
28. Tang, N.; Liu, Y.; Wang, H.; Wu, Z. Mechanism Study of NO Catalytic Oxidation over MnO_x/TiO_2 Catalysts. *J. Phys. Chem. C* **2011**, *115*, 8214–8220. [CrossRef]
29. Sun, W.-y.; Wang, Q.-y.; Ding, S.-l.; Su, S.-j. Simultaneous absorption of SO_2 and NO_x with pyrolusite slurry combined with gas-phase oxidation of NO using ozone: Effect of molar ratio of $O_2/(SO_2+0.5NO_x)$ in flue gas. *Chem. Eng. J.* **2013**, *228*, 700–707. [CrossRef]
30. Mok, Y.S.; Lee, H.-J. Removal of sulfur dioxide and nitrogen oxides by using ozone injection and absorption–reduction technique. *Fuel Processing Technol.* **2006**, *87*, 591–597. [CrossRef]
31. Sun, C.; Zhao, N.; Zhuang, Z.; Wang, H.; Liu, Y.; Weng, X.; Wu, Z. Mechanisms and reaction pathways for simultaneous oxidation of NO_x and SO_2 by ozone determined by in situ IR measurements. *J. Hazard. Mater.* **2014**, *274*, 376–383. [CrossRef]
32. Li, B.; Zhao, J.; Lu, J. Numerical Study of the Simultaneous Oxidation of NO and SO_2 by Ozone. *Int. J. Environ. Res. Public Health* **2015**, *12*, 1595–1611. [CrossRef] [PubMed]
33. Wang, H.; Zhuang, Z.; Sun, C.; Zhao, N.; Liu, Y.; Wu, Z. Numerical evaluation of the effectiveness of NO_2 and N_2O_5 generation during the NO ozonation process. *J. Environ. Sci.* **2016**, *41*, 51–58. [CrossRef] [PubMed]
34. Zou, Y.; Liu, X.; Zhu, T.; Tian, M.; Cai, M.; Zhao, Z.; Wu, H. Simultaneous Removal of NO_x and SO_2 by MgO Combined with O-3 Oxidation: The Influencing Factors and O-3 Consumption Distributions. *ACS Omega* **2019**, *4*, 21091–21099. [CrossRef]
35. Zhou, S.; Zhou, J.; Feng, Y.; Zhu, Y. Marine Emission Pollution Abatement Using Ozone Oxidation by a Wet Scrubbing Method. *Ind. Eng. Chem. Res.* **2016**, *55*, 5825–5831. [CrossRef]
36. Li, Z.; Wuebbles, R.D.; Pylawka, N.J. Rate constant measurement for the reaction of OClO with NO at 220–367 K. *Chem. Phys. Lett.* **2002**, *354*, 491–497. [CrossRef]
37. Johansson, J.; Heijnesson Hultén, A.; Ajdari, S.; Nilsson, P.; Samuelsson, M.; Normann, F.; Andersson, K. Gas-Phase Chemistry of the NO–SO_2–ClO_2 System Applied to Flue Gas Cleaning. *Ind. Eng. Chem. Res.* **2018**, *57*, 14347–14354. [CrossRef]
38. Jin, D.-S.; Deshwal, B.-R.; Park, Y.-S.; Lee, H.-K. Simultaneous removal of SO_2 and NO by wet scrubbing using aqueous chlorine dioxide solution. *J. Hazard. Mater.* **2006**, *135*, 412–417. [CrossRef]
39. Zhang, H.; Ma, D.; Qiu, R.; Tang, Y.; Du, C. Non-thermal plasma technology for organic contaminated soil remediation: A review. *Chem. Eng. J.* **2017**, *313*, 157–170. [CrossRef]
40. Feng, X.; Liu, H.; He, C.; Shen, Z.; Wang, T. Synergistic effects and mechanism of a non-thermal plasma catalysis system in volatile organic compound removal: A review. *Catal. Sci. Technol.* **2018**, *8*, 936–954. [CrossRef]
41. Hong, L.; Chen, D.; Yang, M.; Yin, L.; Wang, D.; Wang, L. Interaction between NO and SO_2 removal processes in a pulsed corona discharge plasma (PCDP) reactor and the mechanism. *Chem. Eng. J.* **2019**, *359*, 1130–1138. [CrossRef]
42. Yamamoto, T.; Okubo, M.; Hayakawa, K.; Kitaura, K. Towards ideal NO_x control technology using a plasma-chemical hybrid process. *IEEE Trans. Ind. Appl.* **2001**, *37*, 1492–1498. [CrossRef]
43. Obradović, B.M.; Sretenović, G.B.; Kuraica, M.M. A dual-use of DBD plasma for simultaneous NO_x and SO_2 removal from coal-combustion flue gas. *J. Hazard. Mater.* **2011**, *185*, 1280–1286. [CrossRef] [PubMed]
44. Wang, T.; Sun, B.M.; Xiao, H.P.; Zeng, J.Y.; Duan, E.P.; Xin, J.; Li, C. Effect of Reactor Structure in DBD for Nonthermal Plasma Processing of NO in N-2 at Ambient Temperature. *Plasma Chem. Plasma Process.* **2012**, *32*, 1189–1201. [CrossRef]
45. Pham, H.-C.; Kim, K.-S. Effect of TiO_2 Thin Film Thickness on NO and SO_2 Removals by Dielectric Barrier Discharge-Photocatalyst Hybrid Process. *Ind. Eng. Chem. Res.* **2013**, *52*, 5296–5301. [CrossRef]
46. Wang, M.; Sun, Y.; Zhu, T. Removal of NO_x, SO_2, and Hg From Simulated Flue Gas by Plasma—Absorption Hybrid System. *IEEE Trans. Plasma Sci.* **2013**, *41*, 312–318. [CrossRef]
47. Huang, L.; Dang, Y. Removal of SO_2 and NO_x by Pulsed Corona Combined with in situ $Ca(OH)_2$ Absorption. *Chin. J. Chem. Eng.* **2011**, *19*, 518–522. [CrossRef]
48. Zhao, L.; Luo, Z.; Jiang, J.; Zhou, D.; Gao, X.; Cen, K. Energy Consumption Analysis and OH Radical Detection of NO Conversion Process From Flue Gas Using Pulsed Corona Discharge. *IEEE Trans. Plasma Sci.* **2014**, *42*, 105–113. [CrossRef]
49. Seo, S.H.; Jo, S.H.; Son, Y.S.; Kim, T.H.; Kim, T.H.; Yu, S. A preliminary study on effect of additive in the removal of NO_x and SO_2 by electron beam irradiation. *Chem. Eng. J.* **2020**, *387*, 124083. [CrossRef]
50. Zhao, L.; Sun, Y.X.; Chmielewski, A.G.; Pawelec, A.; Bulka, S. NO Oxidation with NaClO, $NaClO_2$, and $NaClO_3$ Solution Using Electron Beam and a One Stage Absorption System. *Plasma Chem. Plasma Process.* **2020**, *40*, 433–447. [CrossRef]

51. Chen, R.; Zhang, T.; Guo, Y.; Wang, J.; Wei, J.; Yu, Q. Recent advances in simultaneous removal of SO_2 and NO_x from exhaust gases: Removal process, mechanism and kinetics. *Chem. Eng. J.* **2021**, *420*, 127588. [CrossRef]
52. Zhao, S.; Pudasainee, D.; Duan, Y.; Gupta, R.; Liu, M.; Lu, J. A review on mercury in coal combustion process: Content and occurrence forms in coal, transformation, sampling methods, emission and control technologies. *Prog. Energy Combust. Sci.* **2019**, *73*, 26–64. [CrossRef]
53. Standard Electrode Potential (Data Page). Wikipedia Encyclopedia. Available online: https://encyclopedia.thefreedictionary.com/Standard+electrode+potential+(data+page) (accessed on 12 September 2022).
54. Yi, S.; Liliang, Y.; Haobing, H.; Jiawei, Y.; Shao'an, C. Research trend and practical development of advanced oxdation process on degradation of recalcitrant organic wastewater. *CIESC J.* **2017**, *68*, 1743–1756.
55. Oh, S.-Y.; Kang, S.-G.; Chiu, P.C. Degradation of 2,4-dinitrotoluene by persulfate activated with zero-valent iron. *Sci. Total Environ.* **2010**, *408*, 3464–3468. [CrossRef] [PubMed]
56. Wang, J.; Wang, S. Activation of persulfate (PS) and peroxymonosulfate (PMS) and application for the degradation of emerging contaminants. *Chem. Eng. J.* **2018**, *334*, 1502–1517. [CrossRef]
57. Collins, M.M.; Cooper, C.D.; Dietz, J.D.; Clausen, C.A.; Tazi, L.M. Pilot-scale evaluation of H_2O_2 injection to control to NO_x emissions. *J. Environ. Eng. ASCE* **2001**, *127*, 329–336. [CrossRef]
58. Martinez, N.S.; Fernandez, J.F.; Segura, X.F.; Ferrer, A.S. Pre-oxidation of an extremely polluted industrial wastewater by the Fenton's reagent. *J. Hazard. Mater.* **2003**, *101*, 315–322. [CrossRef]
59. Zhu, Y.; Zhu, R.; Xi, Y.; Zhu, J.; Zhu, G.; He, H. Strategies for enhancing the heterogeneous Fenton catalytic reactivity: A review. *Appl. Catal. B Environ.* **2019**, *255*, 117739. [CrossRef]
60. Lopez-Cueto, G.; Ostra, M.; Ubide, C.; Zuriarrain, J. Fenton's reagent for kinetic determinations. *Anal. Chim. Acta* **2004**, *515*, 109–116. [CrossRef]
61. Liu, Y.; Zhang, J.; Sheng, C.; Zhang, Y.; Zhao, L. Simultaneous removal of NO and SO_2 from coal-fired flue gas by UV/H_2O_2 advanced oxidation process. *Chem. Eng. J.* **2010**, *162*, 1006–1011. [CrossRef]
62. Liu, Y.; Pan, J.; Wang, Q. Removal of Hg-0 from containing-SO_2/NO flue gas by ultraviolet/H_2O_2 process in a novel photochemical reactor. *Aiche J.* **2014**, *60*, 2275–2285. [CrossRef]
63. Guo, R.-T.; Pan, W.-G.; Zhang, X.-B.; Ren, J.-X.; Jin, Q.; Xu, H.-J.; Wu, J. Removal of NO by using Fenton reagent solution in a lab-scale bubbling reactor. *Fuel* **2011**, *90*, 3295–3298. [CrossRef]
64. Hao, R.; Mao, Y.; Mao, X.; Wang, Z.; Gong, Y.; Zhang, Z.; Zhao, Y. Cooperative removal of SO_2 and NO by using a method of UV-heat/H_2O_2 oxidation combined with NH4OH-(NH4)2SO_3 dual-area absorption. *Chem. Eng. J.* **2019**, *365*, 282–290. [CrossRef]
65. Thomas, N.; Dionysiou, D.D.; Pillai, S.C. Heterogeneous Fenton catalysts: A review of recent advances. *J. Hazard. Mater.* **2021**, *404*, 124082. [CrossRef] [PubMed]
66. Li, Y.; Zhang, X.; Lin, H.; Yu, F.; Chen, Z.; Li, C.; Liu, Z.; Yu, J.; Gao, S. The simultaneous removal of SO_2 and NO from flue gas over activated coke in a multi-stage fluidized bed at low temperature. *Fuel* **2020**, *275*, 117862. [CrossRef]
67. Li, J.; Ninh Pham, A.; Dai, R.; Wang, Z.; Waite, T.D. Recent advances in Cu-Fenton systems for the treatment of industrial wastewaters: Role of Cu complexes and Cu composites. *J. Hazard. Mater.* **2020**, *392*, R713–R715. [CrossRef]
68. Wu, B.; Zhang, S.; He, S.; Xiong, Y. Follow-up mechanism study on NO oxidation with vaporized H_2O_2 catalyzed by Fe_2O_3 in a fixed-bed reactor. *Chem. Eng. J.* **2019**, *356*, 662–672. [CrossRef]
69. Matzek, L.W.; Carter, K.E. Activated persulfate for organic chemical degradation: A review. *Chemosphere* **2016**, *151*, 178–188. [CrossRef] [PubMed]
70. Deng, Y.; Ezyske, C.M. Sulfate radical-advanced oxidation process (SR-AOP) for simultaneous removal of refractory organic contaminants and ammonia in landfill leachate. *Water Res.* **2011**, *45*, 6189–6194. [CrossRef] [PubMed]
71. Adewuyi, Y.G.; Khan, M.A.; Sakyi, N.Y. Kinetics and Modeling of the Removal of Nitric Oxide by Aqueous Sodium Persulfate Simultaneously Activated by Temperature and Fe^{2+}. *Ind. Eng. Chem. Res.* **2014**, *53*, 828–839. [CrossRef]
72. Adewuyi, Y.G.; Sakyi, N.Y. Simultaneous Absorption and Oxidation of Nitric Oxide and Sulfur Dioxide by Aqueous Solutions of Sodium Persulfate Activated by Temperature. *Ind. Eng. Chem. Res.* **2013**, *52*, 11702–11711. [CrossRef]
73. Chen, X.; Hu, X. Removal of NO_x and SO_2 from the Coal-Fired Flue Gas Using a Rotating Packed Bed Pilot Reactor with Peroxymonosulfate Activated by Fe(II) and Heating. *Energy Fuels* **2019**, *33*, 6707–6716. [CrossRef]
74. Liu, Y.; Liu, Z.; Wang, Y.; Yin, Y.; Pan, J.; Zhang, J.; Wang, Q. Simultaneous absorption of SO_2 and NO from flue gas using ultrasound/Fe^{2+}/heat coactivated persulfate system. *J. Hazard. Mater.* **2018**, *342*, 326–334. [CrossRef] [PubMed]
75. Antoniou, M.G.; Andersen, H.R. Comparison of UVC/$S_2O_8^{2-}$ with UVC/H_2O_2 in terms of efficiency and cost for the removal of micropollutants from groundwater. *Chemosphere* **2015**, *119*, S81–S88. [CrossRef] [PubMed]
76. Xu, Y.; Lin, Z.; Zhang, H. Mineralization of sucralose by UV-based advanced oxidation processes: UV/PDS versus UV/H_2O_2. *Chem. Eng. J.* **2016**, *285*, 392–401. [CrossRef]
77. Kwon, M.; Kim, S.; Yoon, Y.; Jung, Y.; Hwang, T.-M.; Lee, J.; Kang, J.-W. Comparative evaluation of ibuprofen removal by UV/H_2O_2 and UV/$S_2O_8^{2-}$ processes for wastewater treatment. *Chem. Eng. J.* **2015**, *269*, 379–390. [CrossRef]
78. Wei, Z.; Villamena, F.A.; Weavers, L.K. Kinetics and Mechanism of Ultrasonic Activation of Persulfate: An in Situ EPR Spin Trapping Study. *Environ. Sci. Technol.* **2017**, *51*, 3410–3417. [CrossRef]
79. Si, M.; Shen, B.; Adwek, G.; Xiong, L.; Liu, L.; Yuan, P.; Gao, H.; Liang, C.; Guo, Q. Review on the NO removal from flue gas by oxidation methods. *J. Environ. Sci.* **2021**, *101*, 49–71. [CrossRef] [PubMed]

80. Adewuyi, Y.G.; Sakyi, N.Y. Removal of Nitric Oxide by Aqueous Sodium Persulfate Simultaneously Activated by Temperature and Fe^{2+} in a Lab-scale Bubble Reactor. *Ind. Eng. Chem. Res.* **2013**, *52*, 14687–14697. [CrossRef]
81. Liu, Y.; Wang, Y.; Liu, Z.; Wang, Q. Oxidation Removal of Nitric Oxide from Flue Gas Using UV Photolysis of Aqueous Hypochlorite. *Environ. Sci. Technol.* **2017**, *51*, 11950–11959. [CrossRef] [PubMed]
82. Byoun, S.; Shin, D.N.; Moon, I.-S.; Byun, Y. Quick vaporization of sprayed sodium hypochlorite (NaClO(aq)) for simultaneous removal of nitrogen oxides (NO_x), sulfur dioxide (SO_2), and mercury (Hg0). *J. Air Waste Manag. Assoc.* **2019**, *69*, 857–866. [CrossRef] [PubMed]
83. Wang, Z.; Lun, L.; Tan, Z.; Zhang, Y.; Li, Q. Simultaneous wet desulfurization and denitration by an oxidant absorbent of $NaClO_2/CaO_2$. *Environ. Sci. Pollut. Res.* **2019**, *26*, 29032–29040. [CrossRef] [PubMed]
84. Hao, R.; Yang, S.; Yuan, B.; Zhao, Y. Simultaneous desulfurization and denitrification through an integrative process utilizing $NaClO_2/Na_2S_2O_8$. *Fuel Processing Technol.* **2017**, *159*, 145–152. [CrossRef]
85. Hao, R.; Song, Y.; Tian, Z.; Li, Y.; Zhao, Y.; Wang, Z.; Gong, Y.; Ma, Z.; Qian, Z. Cooperative removal of SO_2 and NO using a cost-efficient triple-area control method. *Chem. Eng. J.* **2020**, *383*, 123164. [CrossRef]
86. Hao, R.; Ma, Z.; Qian, Z.; Gong, Y.; Wang, Z.; Luo, Y.; Yuan, B.; Zhao, Y. New insight into the behavior and cost-effectiveness of different radicals in the removal of NO and Hg0. *Chem. Eng. J.* **2020**, *385*, 123885. [CrossRef]
87. Madia, G.; Koebel, M.; Elsener, M.; Wokaun, A. Side reactions in the selective catalytic reduction of NO_x with various NO_2 fractions. *Ind. Eng. Chem. Res.* **2002**, *41*, 4008–4015. [CrossRef]
88. Hu, Z.; Yang, R.T. 110th Anniversary: Recent Progress and Future Challenges in Selective Catalytic Reduction of NO by H_2 in the Presence of O_2. *Ind. Eng. Chem. Res.* **2019**, *58*, 10140–10153. [CrossRef]
89. Mahmoudi, S.; Baeyens, J.; Seville, J.P.K. NO_x formation and selective non-catalytic reduction (SNCR) in a fluidized bed combustor of biomass. *Biomass Bioenergy* **2010**, *34*, 1393–1409. [CrossRef]
90. Li, G.; Wang, B.; Xu, W.Q.; Li, Y.; Han, Y.; Sun, Q. Simultaneous removal of SO_2 and NO_x from flue gas by wet scrubbing using a urea solution. *Environ. Technol.* **2019**, *40*, 2620–2632. [CrossRef] [PubMed]
91. Gao, F.; Tang, X.; Yi, H.; Zhao, S.; Li, C.; Li, J.; Shi, Y.; Meng, X. A Review on Selective Catalytic Reduction of NO_x by NH_3 over Mn–Based Catalysts at Low Temperatures: Catalysts, Mechanisms, Kinetics and DFT Calculations. *Catalysts* **2017**, *7*, 199. [CrossRef]
92. Liu, Y.; Zhao, J.; Lee, J.M. Conventional and New Materials for Selective Catalytic Reduction (SCR) of NO_x. *Chemcatchem* **2018**, *10*, 1499–1511. [CrossRef]
93. Guan, B.; Zhan, R.; Lin, H.; Huang, Z. Review of state of the art technologies of selective catalytic reduction of NO_x from diesel engine exhaust. *Appl. Therm. Eng.* **2014**, *66*, 395–414. [CrossRef]
94. Yun, B.K.; Kim, M.Y. Modeling the selective catalytic reduction of NO_x by ammonia over a Vanadia-based catalyst from heavy duty diesel exhaust gases. *Appl. Therm. Eng.* **2013**, *50*, 152–158. [CrossRef]
95. Wang, F.; Ma, J.; He, G.; Chen, M.; Zhang, C.; He, H. Nanosize Effect of Al_2O_3 in Ag/Al_2O_3 Catalyst for the Selective Catalytic Oxidation of Ammonia. *ACS Catal.* **2018**, *8*, 2670–2682. [CrossRef]
96. Zhou, J.; Guo, R.-t.; Zhang, X.-f.; Liu, Y.-z.; Duan, C.-p.; Wu, G.-l.; Pan, W.-g. Cerium Oxide-Based Catalysts for Low-Temperature Selective Catalytic Reduction of NO_x with NH_3: A Review. *Energy Fuels* **2021**, *35*, 2981–2998. [CrossRef]
97. Pena, D.A.; Uphade, B.S.; Smirniotis, P.G. TiO_2-supported metal oxide catalysts for low-temperature selective catalytic reduction of NO with NH_3I. Evaluation and characterization of first row transition metals. *J. Catal.* **2004**, *221*, 421–431. [CrossRef]
98. Zhang, Z.; Li, J.; Tian, J.; Zhong, Y.; Zou, Z.; Dong, R.; Gao, S.; Xu, W.; Tan, D. The effects of Mn-based catalysts on the selective catalytic reduction of NO_x with NH_3 at low temperature: A review. *Fuel Processing Technol.* **2022**, *230*, 107213. [CrossRef]
99. Kapteijn, F.; Singoredjo, L.; Andreini, A.; Moulijn, J.A. Activity and selectivity of pure manganese oxides in the selective catalytic reduction of nitric oxide with ammonia. *Appl. Catal. B: Environ.* **1994**, *3*, 173–189. [CrossRef]
100. Han, L.; Cai, S.; Gao, M.; Hasegawa, J.-y.; Wang, P.; Zhang, J.; Shi, L.; Zhang, D. Selective Catalytic Reduction of NO_x with NH_3 by Using Novel Catalysts: State of the Art and Future Prospects. *Chem. Rev.* **2019**, *119*, 10916–10976. [CrossRef] [PubMed]
101. Xiong, S.; Liao, Y.; Xiao, X.; Dang, H.; Yang, S. The mechanism of the effect of H_2O on the low temperature selective catalytic reduction of NO with NH_3 over Mn-Fe spinel. *Catal. Sci. Technol.* **2015**, *5*, 2132–2140. [CrossRef]
102. Mohan, S.; Dinesha, P.; Kumar, S. NO_x reduction behaviour in copper zeolite catalysts for ammonia SCR systems: A review. *Chem. Eng. J.* **2020**, *384*, 123253. [CrossRef]
103. Liu, S.-M.; Guo, R.-T.; Sun, P.; Hu, C.-X.; Wang, S.-X.; Pan, W.-G.; Li, M.-Y.; Liu, S.-W.; Sun, X.; Liu, J. Mechanistic investigation of the different poisoning mechanisms of Cl and P on Mn/TiO_2 catalyst for selective catalytic reduction of NO_x with NH_3. *J. Taiwan Inst. Chem. Eng.* **2017**, *80*, 314–325. [CrossRef]
104. Cai, S.; Hu, H.; Li, H.; Shi, L.; Zhang, D. Design of multi-shell Fe_2O_3@MnO_x@CNTs for the selective catalytic reduction of NO with NH_3:improvement of catalytic activity and SO_2 tolerance. *Nanoscale* **2016**, *8*, 3588–3598. [CrossRef] [PubMed]
105. Zhou, A.; Yu, D.; Yang, L.; Sheng, Z. Combined effects Na and SO_2 in flue gas on $Mn-Ce/TiO_2$ catalyst for low temperature selective catalytic reduction of NO by NH_3 simulated by Na_2SO_4 doping. *Appl. Surf. Sci.* **2016**, *378*, 167–173. [CrossRef]
106. Watling, T.C.; Lopez, Y.; Pless, J.D.; Sukumar, B.; Klink, W.; Markatou, P. Removal of Hydrocarbons and Particulate Matter Using a Vanadia Selective Catalytic Reduction Catalyst: An Experimental and Modeling Study. *SAE Int. J. Engines* **2013**, *6*, 882–897. [CrossRef]

107. Liu, K.J.; Yu, Q.B.; Wang, B.L.; San, J.B.; Duan, W.J.; Qin, Q. Binary copper-manganese based catalysts with urea for low-temperature selective catalytic reduction of NO: Performance, characterization and mechanism. *Appl. Surf. Sci.* **2020**, *508*, 144755. [CrossRef]
108. Tu, B.-S.; Sun, W.; Xue, Y.-J.; Zaman, W.Q.; Cao, L.-M.; Yang, J. Facile Synthesis of PtxNiy Catalyst Supported on Carbon for Low Temperature H_2–SCR. *ACS Sustain. Chem. Eng.* **2017**, *5*, 5200–5207. [CrossRef]
109. Liu, Y.; Tursun, M.; Yu, H.; Wang, X. Surface property and activity of Pt/$Nb2O_5$-ZrO_2 for selective catalytic reduction of NO by H-2. *Mol. Catal.* **2019**, *464*, 22–28. [CrossRef]
110. Wang, X.; Wang, X.; Yu, H.; Wang, X. The functions of Pt located at different positions of HZSM-5 in H-2-SCR. *Chem. Eng. J.* **2019**, *355*, 470–477. [CrossRef]
111. Resitoglu, I.A.; Keskin, A. Hydrogen applications in selective catalytic reduction of NO_x emissions from diesel engines. *Int. J. Hydrog. Energy* **2017**, *42*, 23389–23394. [CrossRef]
112. Cai, X.; Sun, W.; Zaman, W.Q.; Cao, L.; Yang, J. Limited Ce doped Ni–Co as a highly efficient catalyst for H_2-SCR of NO with good resistance to SO_2 and H_2O at low temperature. *RSC Adv.* **2016**, *6*, 91930–91939. [CrossRef]
113. Mrad, R.; Aissat, A.; Cousin, R.; Courcot, D.; Siffert, S. Catalysts for NO_x selective catalytic reduction by hydrocarbons (HC-SCR). *Appl. Catal. A-Gen.* **2015**, *504*, 542–548. [CrossRef]
114. Fu, M.; Li, C.; Lu, P.; Qu, L.; Zhang, M.; Zhou, Y.; Yu, M.; Fang, Y. A review on selective catalytic reduction of NO_x by supported catalysts at 100-300 degrees C-catalysts, mechanism, kinetics. *Catal. Sci. Technol.* **2014**, *4*, 14–25. [CrossRef]
115. Feng, T.; Huo, M.; Zhao, X.; Wang, T.; Xia, X.; Ma, C. Reduction of SO_2 to elemental sulfur with H-2 and mixed H-2/CO gas in an activated carbon bed. *Chem. Eng. Res. Des.* **2017**, *121*, 191–199. [CrossRef]
116. Resitoglu, I.A.; Keskin, A.; Özarslan, H.; Bulut, H. Selective catalytic reduction of NO_x emissions by hydrocarbons over Ag–Pt/Al_2O_3 catalyst in diesel engine. *Int. J. Environ. Sci. Technol.* **2019**, *16*, 6959–6966. [CrossRef]
117. Cheng, X.; Bi, X.T. A review of recent advances in selective catalytic NO_x reduction reactor technologies. *Particuology* **2014**, *16*, 1–18. [CrossRef]
118. Pan, H.; Guo, Y.; Jian, Y.; He, C. Synergistic Effect of Non-thermal Plasma on NO_x Reduction by CH4 over an In/H-BEA Catalyst at Low Temperatures. *Energy Fuels* **2015**, *29*, 5282–5289. [CrossRef]
119. Pekridis, G.; Kaklidis, N.; Komvokis, V.; Athanasiou, C.; Konsolakis, M.; Yentekakis, I.V.; Marnellos, G.E. Surface and Catalytic Elucidation of Rh/γ-Al_2O_3 Catalysts during NO Reduction by C3H8 in the Presence of Excess O_2, H_2O, and SO_2. *J. Phys. Chem. A* **2010**, *114*, 3969–3980. [CrossRef]
120. Gholami, Z.; Luo, G. Low-Temperature Selective Catalytic Reduction of NO by CO in the Presence of O_2 over Cu:Ce Catalysts Supported by Multiwalled Carbon Nanotubes. *Ind. Eng. Chem. Res.* **2018**, *57*, 8871–8883. [CrossRef]
121. Liu, Z.; Wu, J.; Hardacre, C. Research Progress in the Selective Catalytic Reduction of NO_x by H_2 in the Presence of O_2. *Catal. Surv. Asia* **2018**, *22*, 146–155. [CrossRef]
122. Liu, K.; Yu, Q.; Qin, Q.; Wang, C. Selective catalytic reduction of nitric oxide with carbon monoxide over alumina-pellet-supported catalysts in the presence of excess oxygen. *Environ. Technol.* **2018**, *39*, 1878–1885. [CrossRef]
123. Tarjomannejad, A.; Farzi, A.; Niaei, A.; Salari, D. NO reduction by CO over LaB0.5B'O-0.5(3) (B = Fe, Mn, B'=Fe, Mn, Co, Cu) perovskite catalysts, an experimental and kinetic study. *J. Taiwan Inst. Chem. Eng.* **2017**, *78*, 200–211. [CrossRef]
124. Hamada, H.; Haneda, M. A review of selective catalytic reduction of nitrogen oxides with hydrogen and carbon monoxide. *Appl. Catal. A-Gen.* **2012**, *421*, 1–13. [CrossRef]
125. Sreekanth, P.M.; Smirniotis, P.G. Selective Reduction of NO with CO Over Titania Supported Transition Metal Oxide Catalysts. *Catal. Lett.* **2008**, *122*, 37–42. [CrossRef]
126. Kim, H.; Han, B.; Woo, C.G.; Kim, Y. NO_x Removal Performance of a Wet Reduction Scrubber Combined with Oxidation by an Indirect DBD Plasma for Semiconductor Manufacturing Industries. *IEEE Trans. Ind. Appl.* **2018**, *54*, 6401–6407. [CrossRef]
127. Wang, R.; Zhang, X.; Ren, Z. Germanium-based polyoxometalates for the adsorption-decomposition of NO_x. *J. Hazard. Mater.* **2021**, *402*, 123494. [CrossRef] [PubMed]
128. Bélanger, R.; Moffat, J.B. A self-contained catalyst for the reduction of NO_2. *Appl. Catal. B Environ.* **1997**, *13*, 167–173. [CrossRef]
129. Yang, R.T.; Chen, N. A New Approach to Decomposition of Nitric-Oxide Using Sorbent Catalyst Without Reducing Gas—Use of Heteropoly Compounds. *Ind. Eng. Chem. Res.* **1994**, *33*, 825–831. [CrossRef]
130. Belanger, R.; Moffat, J.B. A Comparative-Study of the Adsorption and Reaction Of Nitrogen-Oxides on 12-Tungstophosphoric, 12-Tungstosilicic, and 12-Molybdophosphoric Acids. *J. Catal.* **1995**, *152*, 179–188. [CrossRef]
131. McCormick, R.L.; Boonrueng, S.K.; Herring, A.M. In situ IR and temperature programmed desorption mass spectrometry study of NO absorption and decomposition by silica supported 12-tungstophosphoric acid. *Catal. Today* **1998**, *42*, 145–157. [CrossRef]
132. Zhang, Z.L.; Zhu, L.L.; Ma, J.; Ren, S.L.; Yang, X.Y. Temperature programmed desorption-mass spectrometry study of NO desorption and decomposition by titania supported 12-tungstophosphoric acid. *React. Kinet. Catal. Lett.* **2002**, *76*, 93–101. [CrossRef]
133. Joshi, J.B.; Mahajani, V.V.; Juvekar, V.A. Absorption Of NO_x Gases. *Chem. Eng. Commun.* **1985**, *33*, 1–92. [CrossRef]
134. Thomas, D.; Vanderschuren, J. Nitrogen oxides scrubbing with alkaline solutions. *Chem. Eng. Technol.* **2000**, *23*, 449–455. [CrossRef]
135. Valluri, S.; Kawatra, S.K. Simultaneous removal of CO_2, NO_x and SO_x using single stage absorption column. *J. Environ. Sci.* **2021**, *103*, 279–287. [CrossRef] [PubMed]

136. Yih, S.M.; Lii, C.W. Simultaneous Absorption of Nitric-Oxide and Sulfur-Dioxide in Fe_2—Edta Solutions in a Packed Absorber-Stripper Unit. *Chem. Eng. J. Biochem. Eng. J.* **1989**, *42*, 145–152.
137. Harriott, P.; Smith, K.; Benson, L.B. Simultaneous removal of NO and SO_2 in packed scrubbers or spray towers. *Environ. Prog.* **1993**, *12*, 110–113. [CrossRef]
138. Yih, S.-M.; Lii, C.-W. Absorption of no and SO_2 in Fe(II)-edta solutions I. absorption in a double stirred vessel. *Chem. Eng. Commun.* **1988**, *73*, 43–53. [CrossRef]
139. Yang, L.; Chou, X.-w.; Li, C.; Long, X.-l.; Yuan, W.-k. Reduction of [Fe(III)EDTA]− catalyzed by activated carbon modified with KOH solution. *J. Ind. Eng. Chem.* **2013**, *19*, 784–790. [CrossRef]
140. He, F.; Deng, X.; Chen, M. Evaluation of Fe(II)EDTA-NO reduction by zinc powder in wet flue gas denitrification technology with Fe(II)EDTA. *Fuel* **2017**, *199*, 523–531. [CrossRef]
141. He, F.; Deng, X.; Chen, M. Mechanism and kinetics of Fe(II)EDTANO reduction by iron powder under anaerobic condition. *Fuel* **2016**, *186*, 605–612. [CrossRef]
142. Suchecki, T.T.; Mathews, B.; Augustyniak, A.W.; Kumazawa, H. Applied Kinetics Aspects of Ferric EDTA Complex Reduction with Metal Powder. *Ind. Eng. Chem. Res.* **2014**, *53*, 14234–14240. [CrossRef]
143. He, F.; Qian, Y.; Xu, J. Performance, Mechanism, and Kinetics of Fe(III)EDTA Reduction by Thiourea Dioxide. *Energy Fuels* **2019**, *33*, 3331–3338. [CrossRef]
144. Suchecki, T.T.; Sada, E.; Kumazawa, H. Reduction of (ethylenediaminetetraacetato)iron(III) by sulfite at the boiling temperature. *Ind. Eng. Chem. Res.* **1991**, *30*, 2201–2204. [CrossRef]
145. Suchecki, T.T.; Mathews, B.; Kumazawa, H. Kinetic Study of Ambient-Temperature Reduction of FeIIIedta by $Na_2S_2O_4$. *Ind. Eng. Chem. Res.* **2005**, *44*, 4249–4253. [CrossRef]
146. Liang, C.; Liang, C.-P.; Chen, C.-C. pH dependence of persulfate activation by EDTA/Fe(III) for degradation of trichloroethylene. *J. Contam. Hydrol.* **2009**, *106*, 173–182. [CrossRef] [PubMed]
147. Guo, Q.; He, Y.; Sun, T.; Wang, Y.; Jia, J. Simultaneous removal of NO_x and SO_2 from flue gas using combined Na_2SO_3 assisted electrochemical reduction and direct electrochemical reduction. *J. Hazard. Mater.* **2014**, *276*, 371–376. [CrossRef]
148. Adewuyi, Y.G.; Khan, M.A. Nitric oxide removal by combined persulfate and ferrous–EDTA reaction systems. *Chem. Eng. J.* **2015**, *281*, 575–587. [CrossRef]
149. Adewuyi, Y.G.; Khan, M.A. Nitric oxide removal from flue gas by combined persulfate and ferrous–EDTA solutions: Effects of persulfate and EDTA concentrations, temperature, pH and SO_2. *Chem. Eng. J.* **2016**, *304*, 793–807. [CrossRef]
150. Jastrząb, K. Properties of activated cokes used for flue gas treatment in industrial waste incineration plants. *Fuel Process. Technol.* **2012**, *101*, 16–22. [CrossRef]
151. Liu, Q.; Liu, Z. Carbon supported vanadia for multi-pollutants removal from flue gas. *Fuel* **2013**, *108*, 149–158. [CrossRef]
152. Liu, Z.-S. Adsorption of SO_2 and NO from incineration flue gas onto activated carbon fibers. *Waste Manag.* **2008**, *28*, 2329–2335. [CrossRef] [PubMed]
153. Severa, G.; Head, J.; Bethune, K.; Higgins, S.; Fujise, A. Comparative studies of low concentration SO_2 and NO_2 sorption by activated carbon supported [C2mim] [Ac] and KOH sorbents. *J. Environ. Chem. Eng.* **2018**, *6*, 718–727. [CrossRef]
154. Sumathi, S.; Bhatia, S.; Lee, K.T.; Mohamed, A.R. Cerium impregnated palm shell activated carbon (Ce/PSAC) sorbent for simultaneous removal of SO_2 and NO—Process study. *Chem. Eng. J.* **2010**, *162*, 51–57. [CrossRef]
155. Zhang, Z.; Chen, L.; Wang, J.; Yao, J.; Li, J. Biochar preparation from Solidago canadensis and its alleviation of the inhibition of tomato seed germination by allelochemicals. *RSC Adv.* **2018**, *8*, 22370–22375. [CrossRef]
156. Gao, F.; Tang, X.; Yi, H.; Zhang, B.; Zhao, S.; Wang, J.; Gu, T.; Wang, Y. NiO-Modified Coconut Shell Based Activated Carbon Pretreated with KOH for the High-Efficiency Adsorption of NO at Ambient Temperature. *Ind. Eng. Chem. Res.* **2018**, *57*, 16593–16603. [CrossRef]
157. Shen, Y.F.; Ge, X.L.; Chen, M.D. Catalytic oxidation of nitric oxide (NO) with carbonaceous materials. *Rsc Adv.* **2016**, *6*, 8469–8482. [CrossRef]
158. Guo, Y.; Li, Y.; Zhu, T.; Ye, M. Effects of Concentration and Adsorption Product on the Adsorption of SO_2 and NO on Activated Carbon. *Energy Fuels* **2013**, *27*, 360–366. [CrossRef]
159. Xiong, Y.; Tang, C.; Yao, X.; Zhang, L.; Li, L.; Wang, X.; Deng, Y.; Gao, F.; Dong, L. Effect of metal ions doping (M=Ti^{4+}, Sn^{4+}) on the catalytic performance of MnO_x/CeO_2 catalyst for low temperature selective catalytic reduction of NO with NH_3. *Appl. Catal. A: Gen.* **2015**, *495*, 206–216. [CrossRef]
160. Sumathi, S.; Bhatia, S.; Lee, K.T.; Mohamed, A.R. Selection of best impregnated palm shell activated carbon (PSAC) for simultaneous removal of SO_2 and NO_x. *J. Hazard. Mater.* **2010**, *176*, 1093–1096. [CrossRef] [PubMed]
161. Sumathi, S.; Bhatia, S.; Lee, K.T.; Mohamed, A.R. SO_2 and NO Simultaneous Removal from Simulated Flue Gas over Cerium-Supported Palm Shell Activated at Lower Temperatures−Role of Cerium on NO Removal. *Energy Fuels* **2010**, *24*, 427–431. [CrossRef]
162. Silas, K.; Ghani, W.A.W.A.K.; Choong, T.S.Y.; Rashid, U.; Soltani, S. Regeneration/Optimization of Activated Carbon Monolith in Simultaneous SO_2/NO_x Removal from Flue Gas. *Chem. Eng. Technol.* **2019**, *42*, 1928–1940. [CrossRef]
163. Silas, K.; Ghani, W.A.W.A.K.; Choong, T.S.Y.; Rashid, U. Breakthrough studies of CO_3O_4 supported activated carbon monolith for simultaneous SO_2/NO_x removal from flue gas. *Fuel Process. Technol.* **2018**, *180*, 155–165. [CrossRef]

164. Li, Q.; Hou, Y.; Han, X.; Wang, J.; Liu, Y.; Xiang, N.; Huang, Z. Promotional effect of cyclic desulfurization and regeneration for selective catalytic reduction of NO by NH_3 over activated carbon. *J. Clean. Prod.* **2020**, *249*, 119392. [CrossRef]
165. Zheng, Y.; Kovarik, L.; Engelhard, M.H.; Wang, Y.; Wang, Y.; Gao, F.; Szanyi, J. Low-Temperature Pd/Zeolite Passive NO_x Adsorbers: Structure, Performance, and Adsorption Chemistry. *J. Phys. Chem. C* **2017**, *121*, 15793–15803. [CrossRef]
166. Deng, H.; Yi, H.; Tang, X.; Liu, H.; Zhou, X. Interactive Effect for Simultaneous Removal of SO_2, NO, and CO_2 in Flue Gas on Ion Exchanged Zeolites. *Ind. Eng. Chem. Res.* **2013**, *52*, 6778–6784. [CrossRef]
167. Chiu, C.-H.; Hsi, H.-C.; Lin, C.-C. Control of mercury emissions from coal-combustion flue gases using $CuCl_2$-modified zeolite and evaluating the cobenefit effects on SO_2 and NO removal. *Fuel Process. Technol.* **2014**, *126*, 138–144. [CrossRef]
168. Wang, H.; Yu, Q.; Liu, T.; Xiao, L.; Zheng, X. NO_x storage and reduction with methane by plasma at ambient temperature. *RSC Adv.* **2012**, *2*, 5094–5097. [CrossRef]
169. Wang, H.; Li, X.; Chen, P.; Chen, M.; Zheng, X. An enhanced plasma-catalytic method for $DeNO_x$ in simulated flue gas at room temperature. *Chem. Commun.* **2013**, *49*, 9353–9355. [CrossRef]
170. Vikrant, K.; Kumar, V.; Kim, K.-H.; Kukkar, D. Metal–organic frameworks (MOFs): Potential and challenges for capture and abatement of ammonia. *J. Mater. Chem. A* **2017**, *5*, 22877–22896. [CrossRef]
171. Khan, N.A.; Hasan, Z.; Jhung, S.H. Adsorptive removal of hazardous materials using metal-organic frameworks (MOFs): A review. *J. Hazard. Mater.* **2013**, *244–245*, 444–456. [CrossRef]
172. Murdock, C.R.; Hughes, B.C.; Lu, Z.; Jenkins, D.M. Approaches for synthesizing breathing MOFs by exploiting dimensional rigidity. *Coord. Chem. Rev.* **2014**, *258–259*, 119–136. [CrossRef]
173. Xiao, T.; Liu, D. The most advanced synthesis and a wide range of applications of MOF-74 and its derivatives. *Microporous Mesoporous Mater.* **2019**, *283*, 88–103. [CrossRef]